

Ordovician biostratigraphy: index fossils, biozones and correlation



Daniel Goldman^{1*}, Stephen A. Leslie², Yan Liang³ and Stig M. Bergström⁴

¹Department of Earth and Environmental Geosciences, University of Dayton, 300 College Park, Dayton, OH 45469, USA

²Department of Geology and Environmental Science, James Madison University, MSC 6903, 395 South High Street, Harrisonburg, VA 22807, USA

³State Key Laboratory of Palaeobiology and Stratigraphy, Nanjing Institute of Geology and Palaeontology, Chinese Academy of Sciences, No.39 East Beijing Road, Nanjing 210008, China

⁴School of Earth Sciences, The Ohio State University, 125 South Oval Mall, Columbus, OH 43210, USA

*Correspondence: dgoldman1@udayton.edu

Abstract: Two remarkable events in the history of life on the Earth occur during the Ordovician Period (486.9–443.1 Ma). The first is an exceptionally rapid and sustained radiation of marine life known as the ‘Great Ordovician Biodiversification Event’ (GOBE), and the second is a catastrophic Late Ordovician mass extinction (LOME). Understanding the duration, rate and magnitude of these events requires an increasingly precise global correlation framework. In this chapter we review the major subdivisions of the Ordovician System, their Global Stratotype Section and Points, and the chronostratigraphic levels that define their bases. We also present a detailed set of correlation charts that illustrate the relationships between most of the regional graptolite, conodont and chitinozoan successions across the world.

Supplementary material: Undivided versions of Figures 1, 2 and 3 are available at <https://doi.org/10.6084/m9.figshare.c.6246574>

Introduction

Two remarkable events in the history of life on the Earth occur during the Ordovician Period (486.9–443.1 Ma). The first is an exceptionally rapid and sustained radiation of marine life known as the ‘Great Ordovician Biodiversification Event’ (GOBE), and the second is a catastrophic Late Ordovician mass extinction (LOME). Each of these evolutionary events fundamentally changed the Ordovician marine ecosystem (e.g. see Sheehan 2001; Webby *et al.* 2004b; Harper 2006; Cooper *et al.* 2014; Servais and Harper 2018 and the references therein). Understanding their duration, rate and magnitude requires well-established biostratigraphic zonations that facilitate precise global correlations. Integrating and age dating multi-clade fossil zonal schemes, particularly those from different biofacies, is an important and ongoing task for palaeontologists. Fortunately, the Ordovician has been studied intensely and several groups of marine fossils (primarily graptolites, conodonts and chitinozoans) have the evolutionary (short species durations) and ecological (widespread distribution) characteristics necessary for detailed biostratigraphic zonation

and precise correlation. In this chapter we review the major subdivisions of the Ordovician System, their Global Stratotype Section and Points, and the chronostratigraphic levels that define their bases. We also present a detailed set of correlation charts that illustrate the relationships between most of the regional graptolite, conodont and chitinozoan successions across the world.

The base of the Ordovician Period is defined at the level of the first appearance of the conodont *Iapetognathus fluctivagus* at the Green Point Newfoundland section. Its top, the base of the Silurian Period, is set as the level of the first appearance of the graptolite *Akidograptus ascensus* at Dob’s Linn, Scotland.

Graptolites and conodonts, the two groups used to recognize the levels that define the beginning and end of the Ordovician Period, are also the fossils most often employed for the correlation of Ordovician strata. The stratigraphic ranges of these two groups have been thoroughly studied, and are considered to provide the most precise and reliable data for building widely applicable biostratigraphic zonations. However, recent work has demonstrated the importance and utility of a third group, chitinozoans (Achab 1989; Paris 1990, 1996; Nölvak and

From: Harper, D. A. T., Lefebvre, B., Percival, I. G. and Servais, T. (eds) *A Global Synthesis of the Ordovician System: Part 1*. Geological Society, London, Special Publications, **532**, <https://doi.org/10.1144/SP532-2022-49>

© 2022 The Author(s). This is an Open Access article distributed under the terms of the Creative Commons Attribution License (<http://creativecommons.org/licenses/by/4.0/>). Published by The Geological Society of London. Publishing disclaimer: www.geolsoc.org.uk/pub_ethics

Grahn 1993; Paris *et al.* 2004; Grahn and Nölvak 2007). Graptolite successions are most often described from dark shale sections, particularly those of the outer continental shelf, slope and oceanic settings; conodonts are most commonly extracted from carbonate sections of the shelf and platform, and chitinozoans are found in almost all fine-grained sediments, both shales and limestones.

In some instances, limestone successions have yielded biostratigraphically important graptolites; and conodonts and chitinozoans have been identified from shale surfaces. These uncommon but critically important occurrences have facilitated zonal ties between otherwise disparate biofacies (e.g. Bergström 1986; Goldman *et al.* 2007a, b; Vandembroucke *et al.* 2013). When precisely integrated, these fossil zonations facilitate precise biostratigraphic correlations that can be utilized with confidence across a wide range of facies and latitudes (Bergström 1986; Cooper 1999). Other fossil groups that are useful for regional and inter-regional correlation include trilobites, brachiopods, radiolarians, acritarchs, and, in Upper Ordovician carbonate facies, corals and stromatoporoids (Webby *et al.* 2004a, b; Pouille *et al.* 2014; Servais *et al.* 2017).

Evolution and ecology of key index fossil clades

Graptolites

The Graptolithina comprise the colonial members of the Class Pterobranchia (Phylum Hemichordata), and include both benthic and planktic groups. Recent phylogenetic analyses have suggested that the Graptolithina is not an extinct clade, and that the extant genus *Rhabdopleura* is a ‘living’ benthic graptolite (Mitchell *et al.* 2013). Planktic graptolites (Order Graptoloidea) are known only from the fossil record, and are the taxa used for Ordovician biozonation and correlation. The evolutionary origin of planktic graptoloids (from here on referred to as graptolites) is not well understood but is considered to lie among members of the Middle–Upper Cambrian Dendrograptidae (Maletz 2019). The first graptoloid species to appear in the earliest Ordovician is *Rhabdinopora proparabola* (Maletz *et al.* in press), and it provides a useful marker for the lowermost Ordovician in clastic facies that do not yield conodonts.

Graptolites were a major component of the Ordovician macroplankton and represent the first substantial fossil record of zooplankton. They lived at various depths in the ocean waters (Chen 1990; Cooper *et al.* 1991, 2012, 2017; Chen *et al.* 2001), were particularly abundant along continental margins in upwelling zones (Fortey and Cocks 1986; Finney and Berry 1997) and are found in a wide range of

sedimentary facies, although most are abundant in distal shelf/slope deposits.

Many graptolite species spread rapidly after origination, are widespread globally and have relatively short stratigraphic durations, lasting for 2 myr or less. It is estimated (Foote *et al.* 2019) that the published graptoloid record captures up to 75% of the original species richness and, on average, 85% of the original durations for species known from more than one collection. These attributes combine to make graptolites extremely valuable fossils for subdividing and correlating Ordovician and Silurian strata (Skevington 1963; Cooper and Lindholm 1990; Webby *et al.* 2004a; Cooper and Sadler 2012; Loydell 2012; Maletz 2021).

Conodonts

Conodonts represent an extinct microfossil group whose phylogenetic relationships remain controversial. The main reason for this is the fact that complete specimens (including soft tissue) are exceedingly rare in the fossil record and the few found have been the subject of different interpretations. Although common in rocks of Cambrian–Triassic age, as a rule they occur only as parts of the phosphatic-feeding apparatus and complete assemblages of such apparatuses are quite uncommon. Most species are known only from isolated denticles from the feeding apparatus. These isolated denticles are referred to as conodont elements.

Most conodont elements have a size of less than 1 mm but specimens up to a size of several millimetres are known. The size of the conodont animal appears to have had a considerable range from a few centimetres up to perhaps 0.5 m. The global distribution of many taxa in a variety of marine environments suggests that they were active swimmers, although it has been suggested that at least some taxa were parasitic. Most authors interpret conodonts as primitive vertebrates (e.g. Aldridge *et al.* 1993, 2013; Donoghue *et al.* 2000, 2008) but others suggest that they belong to an isolated group of marine fossils. Their widespread occurrence in rocks deposited in a wide variety of environments indicates that they were an important and very common part of the marine faunas.

Because of the phosphatic composition of the conodont elements, they can be isolated from calcareous marine rocks by acid treatment or by the boiling of soft shales in water. Conodont elements also occur on bedding surfaces of hard graptolite shales from which they are not easily isolated. Extensive work on conodonts extracted from limestone samples has resulted in the establishment of detailed conodont zonations of Ordovician successions in several regions of the world (e.g. Bergström 1971), which has made these microfossils very valuable for both

Ordovician biozonation

short- and long-distance correlations. Together with graptolites, they are currently the biostratigraphically most globally useful Ordovician index fossils.

Chitinozoans

Chitinozoans are an extinct group of organic-walled microfossils that are abundant in Lower–Middle Paleozoic strata. They have bottle-shaped, radially symmetrical organic-walled tests with an opening sealed with an apertural plug (either operculum or prosome). Their taxonomic affinity is unknown but multiple hypotheses have been proposed to explain their biological origin, including classification as protists (e.g. Eisenack 1931, 1932; Collinson and Schwalb 1955; Obut 1973; Reid and John 1981; Cashman 1990, 1991), fungi (Locquin 1981) and a new but hitherto unknown group (Bockelie 1981). The most prevailing hypothesis for the last four decades is that chitinozoans are the eggs or egg capsules of cryptic metazoans (e.g. Kozlowski 1963; Grahn 1980; Paris 1981; Jaglin and Paris 1992; Paris and Nölvak 1999; Grahn and Paris 2011). However, recent work carried out by Liang *et al.* (2019, 2020) on the magnitude of size variations in chitinozoan populations, and on exceptionally preserved specimens fossilized during reproduction, has questioned the egg hypothesis. Liang *et al.* (2020) proposed that chitinozoans most plausibly represent a new, isolated group of protists.

Along with graptolites and conodonts, chitinozoans have been studied intensely and utilized in high-resolution Ordovician–Silurian biostratigraphy (Achab 1989; Paris 1990, 1996; Nölvak and Grahn 1993; Paris *et al.* 2004; Grahn and Nölvak 2007). They are generally considered to be planktic or epiplanktic (Paris 1996; Paris and Verniers 2005) and have been recovered in almost all types of sediments, from shallow-water deposits to outer-shelf and slope sediments (although there are no firm occurrences recorded from abyssal deposits). These widespread occurrences indicate that chitinozoans were not strongly controlled by environmental factors, and thus could be used as an efficient tool in biostratigraphy. Chitinozoans were thought to have their greatest overall abundance on the shelf, which then diminishes towards both shallower and deeper water (Paris and Verniers 2005), but case studies are limited and more comprehensive data are required to better demonstrate this issue. Chitinozoans are commonly isolated from carbonates by acid dissolution but important work on extracting specimens from black shale (e.g. see Achab 1980; Paris 1981; Vandenbroucke *et al.* 2005, 2013; Achab and Maletz 2022) has improved correlation across biofacies and added important data to some long-standing stratigraphic problems in Ordovician stratigraphy.

Subdivision of the Ordovician System

Many fossil faunas exhibited strong biogeographical differentiation during the Lower Paleozoic, particularly in the Ordovician. Historically, because of the strong faunal provincialism and facies differentiation that existed throughout most of the Ordovician, no regional suite of stages or series proved entirely satisfactory for global application. Therefore, the Ordovician Subcommission determined that a set of globally applicable set of chronostratigraphic (and chronological) units defined by fossil-based levels that had the potential for precise widespread correlation needed to be developed (Webby 1995, 1998).

The International Commission on Stratigraphy (ICS) recognized a three-fold subdivision of the Ordovician System (Webby 1995): the Lower, Middle and Upper Ordovician Series. Seven chronostratigraphic levels were established as primary correlation levels for seven international stages. These stage boundaries are based on the first appearance of key graptolite or conodont species, have been formally voted on, and are defined by a Global Boundary Stratigraphic Section and Point (GSSP). From the oldest to youngest, they are Tremadocian, Floian, Dapingian, Darriwilian, Sandbian, Katian and Hirnantian (Figs 1a–e, 2a–e & 3a–e).

A short review of how the stage boundary levels are recognized is provided below. Photographs of the key index taxa whose first appearance marks the level of the GSSPs for the Floian (*Paratetrograptus approximatus*), Sandbian (*Nemagraptus gracilis*) and Hirnantian (*Metabolograptus extraordinarius*) stages are shown in Figures 4, 5 and 6, respectively. These graptolite species were not illustrated in the 2020 revision of the geological timescale (Goldman *et al.* 2020).

The Tremadocian Stage

The GSSP for the base of the Tremadocian Stage, the Lower Ordovician Series and the Cambrian–Ordovician boundary is in the Green Point section of western Newfoundland. The boundary is defined as the level of the first appearance of the conodont species *Iapetognathus fluctivagus* in Bed 23, in the lower Broom Point Member of the Green Point Formation, 4.8 m below the first appearance level of the planktic graptolite *Rhabdinopora preparabola* in Bed 25 (cf. Cooper *et al.* 2001). The relatively close similarity of the oldest occurrence of these widespread key taxa also made it possible to recognize the Cambrian–Ordovician boundary level in successions lacking conodonts.

However, it is appropriate to note that there is currently some controversy regarding the taxonomy and appearance level of *I. fluctivagus* at the GSSP.

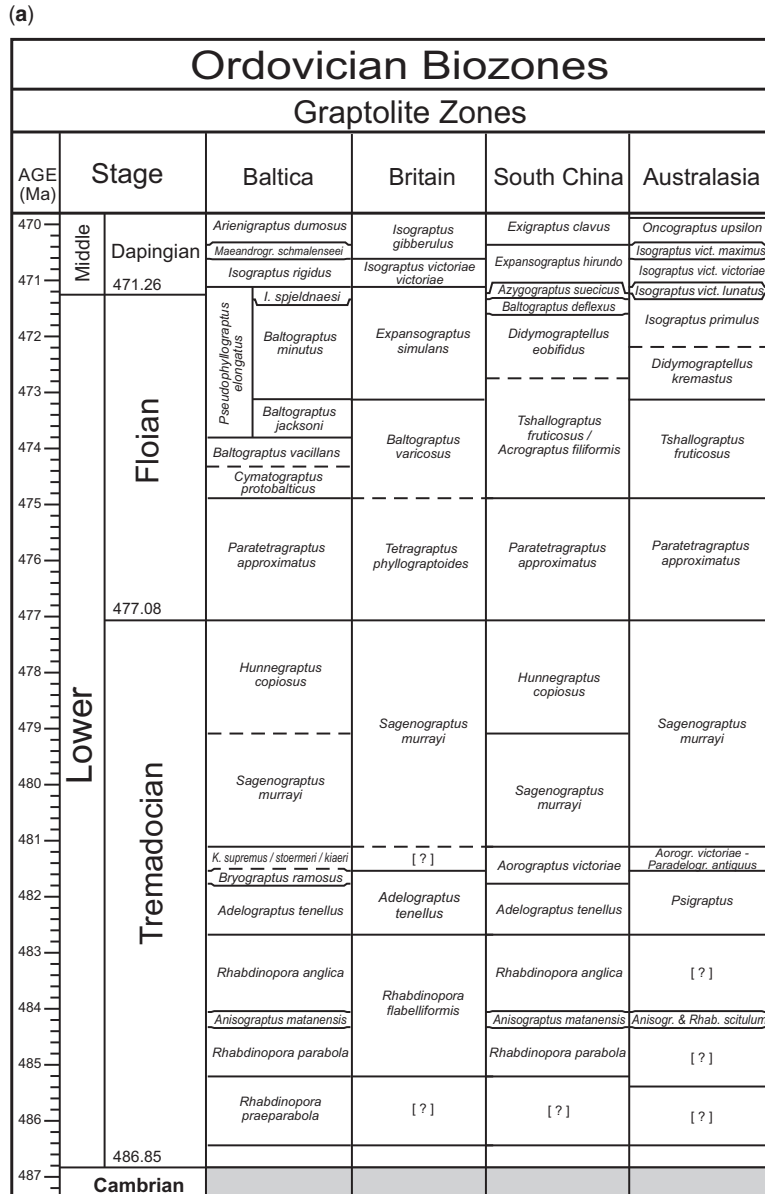


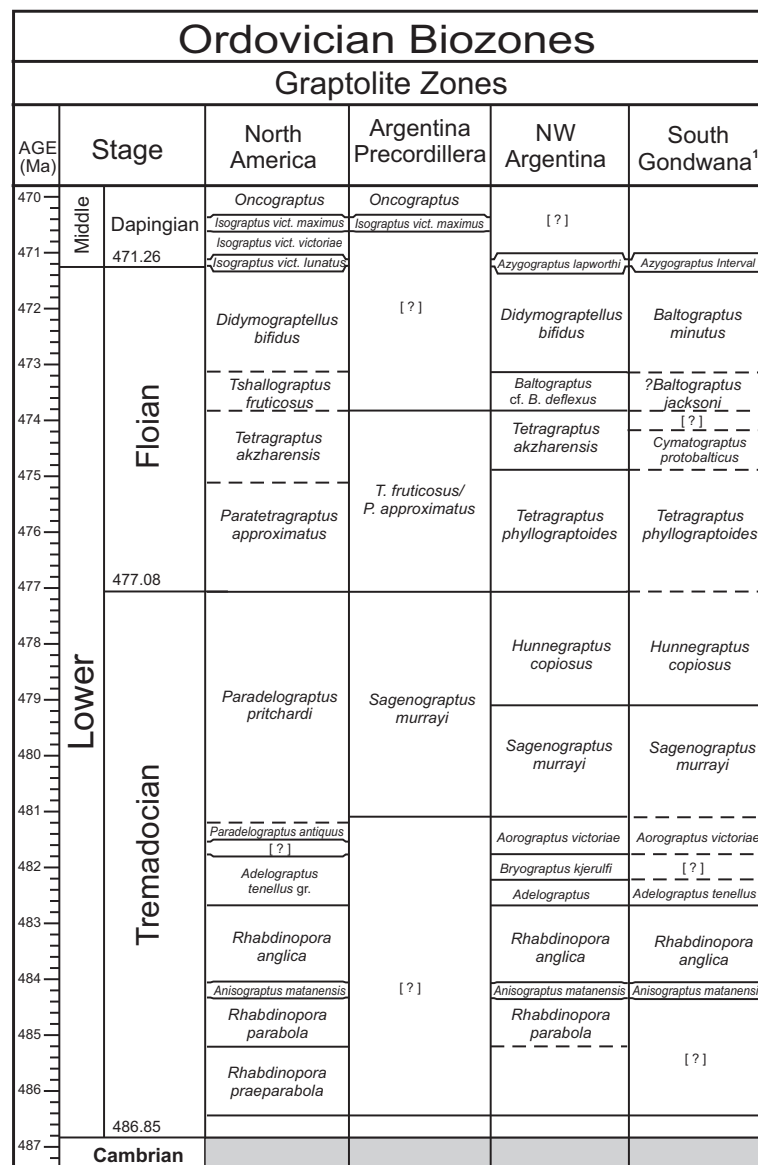
Fig. 1. (a)–(e) Lower Ordovician timescale, stages, and graptolite, conodont and chitinozoan zonal schemes. The leftmost column is the chronometrical timescale from Goldman *et al.* (2020, in Gradstein *et al.* 2020). Zonations and correlations for graptolites are modified from the following (and references therein): Vandenberg and Cooper (1992), Zalasiewicz *et al.* (2009), Cooper and Sadler (2012), Loydell (2012), Maletz and Ahlberg (2018), Hererra Sánchez *et al.* (2019), Goldman *et al.* (2020) and Maletz (2021); for conodonts they are modified from Bergström and Wang (1995), Zhen and Percival (2003), Zhen *et al.* (2015, 2017), Zhen (2021), Albanesi and Ortega (2016), Z. H. Wang *et al.* (2019), Zhang *et al.* (2019) and Goldman *et al.* (2020); and for chitinozoans from Paris *et al.* (2004), Nölvak *et al.* (2006) and Goldman *et al.* (2020).¹ The South Gondwana graptolite zonation for the Lower Ordovician is adapted from Gutiérrez-Marco and Martin (2016).

According to Terfelt *et al.* (2012), the *Iapetognathus* specimens in Bed 23 belong rather to *I. praengensis*, and this latter species also occurs below Bed

23 in the Green Point succession. Other authors, however, do not agree with this interpretation (Miller *et al.* 2014).

Ordovician biozonation

(b)

**Fig. 1. Continued.**

Miller *et al.* (2014) refuted many of Terfelt *et al.*'s (2012) stratigraphic and taxonomic interpretations, including the level at which the various species of *Iapetognathus* appear (see Stouge *et al.* 2017). In order to acknowledge the ongoing research and discussion related to this important boundary level, and to facilitate its precise international correlation, the Ordovician Subcommission approved two Auxiliary Stratotype Sections and Points

(ASSPs) for the base of the Ordovician System. These are the Lawson Cove Section, Ibex area, Utah, USA (Miller *et al.* 2016) and the Xiaoyangqiao section at Dayangcha, North China (Wang *et al.* 2021).

Other useful but less known index fossils found in the Green Point succession are radiolarians, which occur in the upper part of Beds 23, 25 and 26, and represent the *Protoentictinia kuzuriana*

(c)

Ordovician Biozones					
AGE (Ma)	Stage	Chitinozoan Zones		Conodont Zones	
		Baltica	North Gondwana	Baltica	N. America Midcontinent
470	Lower Tremadocian	Euconochitina primitiva	Belonechitina henryi	<i>M. parva</i>	<i>Histiodella altifrons</i>
471	Middle		<i>Paroisto. originalis</i>		
471.26	Dapingian		<i>Desmochitina ornensis</i>	<i>Baltoniodus navis</i>	<i>Microzarkodina flabellum / Tripodus laevis</i>
471.26	471.26		<i>Baltoniodus triangularis</i>		
472	<i>Eremochitina brevis</i>		<i>Oepikodus evae</i>	<i>Reutterodus andinus</i>	
473					
474	<i>Eremochitina baculata</i>		<i>Prioniodus elegans</i>	<i>Oepikodus communis</i>	
475	<i>Euconochitina symmetrica</i>		<i>Paroistodus proteus</i>	<i>Acodus deltatus / Oneotodus costatus</i>	
476					
477					477.08
478	<i>Lagenochitina confundens</i>				
479	<i>Lagenochitina destombesi</i>		<i>Paltodus deltifer</i>	<i>Macerodus dianae</i>	
480					
481					
482	<i>Lagenochitina destombesi</i>		<i>Cordyliodus angulatus</i>	<i>Scolopodus subrex</i>	
483				<i>Rossodus manitouensis</i>	
484				<i>Cordyliodus angulatus</i>	
485	<i>Iapetognathus fluctivagus</i>		<i>Iapetognathus fluctivagus</i>	<i>Iapetognathus fluctivagus</i>	
486					486.85
487					Cambrian

Fig. 1. Continued.

Assemblage (Won *et al.* 2005; Pouille *et al.* 2014). The radiolarians may be useful for correlation of the boundary in slope facies sections.

Trilobites and other shelly fossils are not common in the systemic boundary interval at the GSSP. However, trilobite species belonging to *Sympshurina* have been found in Bed 25 just below the first appearance datum (FAD) of *R. praeparabolus* (Stouge *et al.* 2017). These fossils provide a

straightforward correlation into the western Laurentian platform sections, which also contain the trilobite *Jujuyapsis borealis*, species of *Sympshurina* (Loch and Taylor 2012) and *I. fluctivagus*.

The upper and lower boundaries of the Tremadocian Stage correlate well with those of the British Tremadoc Series (Rushton 1982). The name was approved by the ICS in 1999 (Cooper and Sadler 2012).

Ordovician biozonation

(d)

Ordovician Biozones						
AGE (MA)	Stage	Conodont Zones				
		N. China	S. China (platform)	S. China (slope)	Kazakhstan	
470	Floian	[?]	<i>M. parva</i>	<i>Paroistodus originalis</i>	<i>Periodon cf. P. hankensis</i>	
471			<i>Paroisto. originalis</i>	[?]		
472		<i>Jumudontus ganada</i>	<i>Baltoniodus navis</i>	<i>Oepikodus evae</i>		
473		<i>Paraserratognathus obesus/ Paraserratognathus peltoidiformis</i>	<i>Balton. triangularis</i>			
474			<i>Oepikodus evae</i>		<i>Oepikodus evae</i>	
475			<i>Oepikodus communis</i>			
476		<i>Serratognathus extensus</i>	<i>Prioniodus honghuayuanensis</i>	<i>Prioniodus elegans</i>	<i>Prioniodus elegans</i>	
477			<i>Serratognathus bilobatus</i>	<i>Serratognathus diversus</i>	<i>Prioniodus oepiki</i>	
478	Tremadocian	<i>Scalpellodus ergus</i>	<i>Triangulodus bifidus</i>	<i>Triangulodus bifidus</i>	<i>Acodus longibasis</i>	
479			<i>Colaptoconus quadruplicatus</i>	<i>Paroistodus proteus</i>		
480		<i>Triangulodus proteus / Colaptoconus quadruplicatus</i>			<i>Rossodus manitouensis</i>	
481		<i>Paltodus deltifer</i>	<i>Chosonodina herfurthi</i>			
482			<i>Rossodus manitouensis</i>	<i>Cordylodus angulatus</i>		
483		<i>Chosonodina herfurthi</i>	<i>Cordylodus angulatus</i>		<i>Iapetognathus fluctivagus</i>	
484		<i>Cordylodus angulatus</i>				
485		<i>Cordylodus lindstromi / Iapetognathus fluctivagus</i>	<i>Monocostodus sevierensis</i>	<i>Cordylodus lindstromi</i>		
486						
487						
Cambrian						

Fig. 1. Continued.

The Floian Stage

In the current classification of the Ordovician System, the second stage above its base is the Floian Stage. This unit received its name from the Village of Flo, which is located about 5 km SE of the Floian GSSP, which is at Diabasbrottet. This GSSP is located about 80 km NNW of the city of Göteborg and 12 km SE of the town of Vänersborg in the province of Västergötland in southwestern Sweden. The

Diabasbrottet Quarry, long inactive, is located on the northwestern slope of Mount Hunneberg (Maletz *et al.* 1996; Bergström *et al.* 2004, 2019).

At the Diabasbrottet GSSP, the succession consists of the Tøyen Shale, which is a black shale with some, generally thin, beds of dense fossiliferous limestone. The black shale contains numerous graptolites and the limestone beds have yielded taxonomically diverse conodonts. At its GSSP, the base of the Floian Stage, now marked by a ‘golden spike’, is

(e)

		Ordovician Biozones			
AGE (MA)	Stage	Conodont Zones			
		Argentina Precordillera	NW Argentina	Australia (platform)	E. Australia (slope-basinal)
470	Middle Dapingian	<i>M. parva</i>	[?]		
471	471.26	<i>Baltoniodus navis</i>	<i>Baltoniodus 'navis'</i>		
		<i>Balton. triangularis</i>	<i>Balton. triangularis</i>	<i>Jumudentus ganada</i>	<i>Periodon hankensis</i>
472		<i>Oepikodus intermedius</i>	<i>Baltoniodus cf. triangularis</i>	<i>O. evae</i>	[?]
473		<i>Oepikodus evae</i>	<i>Trapez. diprion</i>		<i>Oepikodus evae</i>
			<i>Gothodus andinus</i>		
474		<i>Prioniodus elegans</i>	<i>Oepikodus communis</i>	<i>Oepikodus communis</i>	[?]
475			<i>Tropodus sweeti</i>		
476				<i>Serralognathus bilobatus/ Prioniodus oepiki</i>	<i>Paracordyliodus gracilis</i>
477	477.08	<i>O. elongatus /A. deltatus</i>	<i>Acodus triangularis</i>	<i>Paroistodus proteus</i>	<i>Prioniodus oepiki</i>
478					[?]
479		<i>Paroistodus proteus</i>			
480		<i>Stiptognathus borealis</i>	<i>Paroistodus proteus/ Acodus apex</i>		
481					
482		<i>Macerodus dianae</i>	<i>P. deltifer</i>		
		<i>Paltodus deltifer</i>	<i>P. d. deltifer</i>		
			<i>P. d. pristinus</i>		
483					
484		<i>Cordyliodus angulatus</i>	<i>Cordyliodus angulatus</i>	[?]	[?]
485					
486		<i>Iapetognathus fluctivagus</i>	<i>Iapetognathus fluctivagus</i>		
487	486.85				
	Cambrian				

Fig. 1. Continued.

placed at the level of the first appearance of the globally distributed graptolite *Paratetrograptus approximatus* (Fig. 4). This biostratigraphic level can be widely recognized throughout low- to middle-palaeolatitude regions where it commonly includes the FAD of *Tetragraptus phyllograptoides*, which also debuts in the GSSP horizon at Diabasbrottet. *Tetragraptus phyllograptoides* is well known from high-latitude localities (e.g. the Central Andean Basin; see Herrera Sánchez *et al.* 2019) and, hence, a precise correlation of the boundary level can be

traced through graptolite successions around the world.

In terms of conodont biostratigraphy, this level is a little above the base of the *Oelandodus elongatus–Acodus deltatus* Subzone of the *Paroistodus proteus* Zone of the Baltoscandian (mid-palaeolatitude) succession (Löfgren 1993; Maletz *et al.* 1996; Bergström *et al.* 2004). In the North American Midcontinent (low-latitude) succession, this level is close to the base of the *A. deltatus–Oneotodus costatus* Zone; and in North China and the Canning Basin

Ordovician biozonation

(a)

Ordovician Biozones						
Graptolite Zones						
AGE (Ma)	Stage	Baltica	Britain	South China	Australasia	
457	Upper Middle	Dariilian	Didymograptus artus	Nemagraptus gracilis	Nemagraptus gracilis	Nemagraptus gracilis
458				Jiangxigraptus vagus	Hustedograptus teretiusculus	Jiangxigraptus vagus
459				Pseudoplexograptus distichus	Didymograptus murchisoni	Didymograptus murchisoni
460				Pterograptus elegans	Pterograptus elegans	Archiclimacograptus riddellensis
461				Nicholsonograptus fasciculatus	Nicholsonograptus fasciculatus	
462				Holmograptus latus	Acrograptus ellesae	
463				Eoglyptograptus cumbrensis	Levisograptus intersitus	
464				Levisograptus austrodentatus	Levisograptus austrodentatus	Levisograptus austrodentatus
465				Ariegraptus dumosus/ Pseudograptus manubriatus	Isograptus gibberulus	Cardiograptus morsus
466				Maeandograptus schmalenseei	Exigograptus clavus	Oncograptus uppsilon
467	Lower	Dapingian	Isograptus rigidus	Isograptus rigidus	Expansograptus hirundo/ P. caducus imitatus	Isograptus vinct. maximus
468				Isograptus rigidus	Azygograptus suecicus	Isograptus vinct. victoriae
469				P. elongatus	Baltograptus deflexus	Isograptus v. lunatus
470				Isograptus rigidus	Didymograptellus eobifidus	Isograptus primulus
471	Floian	P. elongatus	Isograptus spjeldnaesi	Baltograptus minutus		
472						

Fig. 2. (a)–(e) Middle Ordovician timescale, stages, and graptolite, conodont and chitinozoan zonal schemes. The leftmost column is the chronometrical timescale from Goldman *et al.* (2020, in Gradstein *et al.* 2020). Zonations and correlations for graptolites are modified from the following (and references therein): Vandenberg and Cooper (1992), Zalasiewicz *et al.* (2009), Cooper and Sadler (2012), Loydell (2012), Maletz and Ahlberg (2018), Goldman *et al.* (2020) and Maletz (2021); for conodonts they are modified from Bergström and Wang (1995), Zhen and Percival (2003), Zhen and Nicoll (2009), Albanesi and Ortega (2016), Z. H. Wang *et al.* (2019), Zhang *et al.* (2019), Goldman *et al.* (2020) and Zhen *et al.* (2020a, b), Zhen (2021); and for chitinozoans from Goldman *et al.* (2020). ¹The South Gondwana graptolite zonation for the Middle Ordovician is adapted from Gutiérrez-Marco *et al.* (2017).

in Australia, this level is near the base of the *Serratognathus bilobatus* Zone (Zhen *et al.* 2017; Z.H. Wang *et al.* 2019). In Baltoscandia, this level is also within the *Megistaspis (Paramegistaspis) planilimbata* Trilobite Zone. In 2002, the ICS ratified the GSSP for the Floian Stage and the stage was named in 2005. This biostratigraphic level was also adopted

for the base of the revised British Arenig Series (Fortey *et al.* 1995).

The Dapingian Stage

The GSSP for the base of the Dapingian Stage and the base of the Middle Ordovician Series is the

(b)

Ordovician Biozones						
Graptolite Zones						
AGE (Ma)	Stage	North America	Argentina Precordillera	NW Argentina	South Gondwana ¹	
457	Middle Darriwilian	Late Sandbian	<i>Nemagraptus gracilis</i>	<i>Nemagraptus gracilis</i>	[?]	<i>Orthograptus bekkeri</i>
458		458.18	<i>Hustedograptus teretiusculus</i>	<i>Hustedograptus teretiusculus</i>	<i>Hustedograptus teretiusculus</i>	<i>Hustedograptus teretiusculus</i>
459			[?]	[?]		
460						
461						<i>Pseudoplex distichus</i>
462						
463			<i>Pterograptus elegans</i>	<i>Pterograptus elegans</i>		
464					[?]	
465			<i>Nicholsonograptus fasciculatus</i>	[?]		
466						
467	Dapingian		<i>Holmograptus spinosus</i>	<i>Holmograptus spinosus</i>		<i>Didymograptus artus / Didymograptus spinulosus</i>
468			<i>Holmograptus lenticulus</i>	<i>Holmograptus lenticulus</i>		
469		469.42	<i>Levisograptus dentatus</i>	<i>Levisograptus dentatus</i>	<i>Levisograptus dentatus</i>	<i>Corymbograptus retroflexus</i>
470			<i>Oncograptus</i>	<i>Cardiograptus</i>	[?]	[?]
471		471.26	<i>Isograptus vinct. maximum</i>	<i>Isograptus vinct. maximum</i>		<i>Expansograptus hirundo</i>
472	Lower Floian		<i>Isograptus vinct. victoriae</i>			
			<i>Isograptus vinct. lunatus</i>			
			<i>Didymograptellus bifidus</i>			

Fig. 2. Continued.

stratigraphic level of the FAD of the conodont *Baltoniodus triangularis*, which is 10.57 m above the base of the Dawan Formation at the base of Bed SHOD-16 in the Huanghuachang section, 22 km NE of Yichang city, Hubei Province, South China (Wang *et al.* 2009). The FAD of the conodont *Microzarkodina flabellum* occurs 0.2 m above this horizon. The conodont succession across the Lower–Middle Ordovician boundary records important speciation events in the *Baltoniodus*, *Gothodus*, *Microzarkodina* and *Periodon* lineages. The appearance of these new taxa, which dispersed rapidly,

enables the correlation of the GSSP into conodont successions where *B. triangularis* is uncommon.

Based on the graptolite succession from the Huanghuachang section, X.F. Wang *et al.* (2009) and C.H. Wang *et al.* (2013) placed the base of the Dapingian Stage close to the boundary between the lower and upper *Azygograptus suecicus* Zone (as defined by the first appearance of *Azygograptus ellesii*). X.F. Wang *et al.* (2009) correlated the GSSP level with the North Gondwana *Belonechitina henryi* Chitinozoan Zone and noted that it also falls within the *Ampullulae*–*Barakella felix* acritarch assemblage zone.

Ordovician biozonation

(c)

Ordovician Biozones							
AGE (Ma)	Stage		Chitinozoan Zones		Conodont Zones		
			Baltica	North Gondwana	Baltica	N. America Midcontinent	
457	Upper Sandbian 458.18	Darijilian	Laufeldochitina stentor	<i>Lagenochitina deunfti</i>	<i>Baltoniodus variabilis</i>	<i>Plectodina aculeata</i>	
458				<i>Lagenochitina ponctif.</i>	<i>Pygodus anserinus</i>	<i>Cahabagnathus sweeti</i>	
459				<i>Lirochitina pissotensis</i>			
460				<i>Laufeldochitina clavata</i>	<i>Pygodus serra</i>	<i>Cahabagnathus friendsvillensis</i>	
461				<i>Armoricochitina americana - Cyathochitina jenkinsi</i>			
462			Laufeldochitina striata		<i>Pygodus anitae</i>	<i>Histiodella bellburnensis</i>	
463					<i>Pygodus lunensis</i>	<i>Histiodella kristinae</i>	
464					<i>Eoplacognathus suecicus</i>		
465					<i>Eoplacognathus pseudoplanus</i>		
466	Middle Dapingian 469.42	471.26	Cyathochitina regnelli	<i>Siphonochitina ormosa</i>	<i>Yangtze-placognathus crassus</i>	<i>Histiodella holodenata</i>	
467				<i>Cyathochitina calix - protocalix</i>			
468				<i>Desmochitina bulla</i>			
469				<i>Conochitina cucumis</i>	<i>Lenodus variabilis</i>	<i>Histiodella sinuosa</i>	
470				Euconochitina primativa	<i>L. antivariabilis</i>	<i>Histiodella altifrons</i>	
471			Floian		<i>Microzarkodina parva</i>		
472					<i>Paroisto. originalis</i>		
					<i>Baltoniodus navis</i>	<i>Microzarkodina flabellum / Tripodus laevis</i>	
					<i>Balton. triangularis</i>		
			<i>Eremochitina brevis</i>	<i>Oepikodus evae</i>	<i>Reutterodus andinus</i>		

Fig. 2. Continued.

Correlation of the conodont-defined Dapingian Stage GSSP into graptolite-bearing sections devoid of conodonts is facilitated by the co-occurrence of graptolites and conodonts in the Huanghuachang section itself (X.F. Wang *et al.* 2009; C.H. Wang *et al.* 2013), as well as in the Cow Head Group of western Newfoundland (Williams and Stevens 1988; Stouge 2012) and the Trail Creek region of Idaho, western USA (Goldman *et al.* 2007b). There are, however, some differences in the recent literature regarding the correlation of the base of the Dapingian Stage with graptolite-bearing successions. X.F. Wang *et al.* (2009) and C.H. Wang *et al.* (2013) correlated the GSSP level with the

base of the *Isograptus victoriae victoriae* Zone (Ca2 in the Australasian zonation) but recent work by Zhen *et al.* (2020b) suggests that the base of the Dapingian Stage could correlate with a slightly younger level that is closer to the base of the *Isograptus victoriae maximus* Zone (Ca3). Herrera Sánchez *et al.* (2019) and Toro *et al.* (2020) correlated the basal Dapingian with the *Azygograptus lapworthi* Biozone of the Central Andean Basin, which was then succeeded by a slightly younger first appearance of *I. victoriae*.

These small differences notwithstanding, the base of the Dapingian Stage and the Middle Ordovician can be recognized and globally correlated with

(d)

Ordovician Biozones									
AGE (Ma)	Conodont Zones								
	Stage	N. China	S. China (platform)	S. China (slope)	Kazakhstan				
457	Upper Sandbian	Plectodina aculeata	Baltoniodus variabilis	Pygodus anserinus	Pygodus anserinus	Pygodus anserinus			
458		Pygodus anserinus	Yangtzeplacognathus jianyeensis / Pygodus anserinus						
459		Pygodus serra	Pygodus serra	Pygodus serra	Pygodus serra				
460		Eoplacognathus suecicus / Histiodella kristinae	Eoplacognathus suecicus	Histiodella kristinae	Periodon aculeatus				
461		Tangshanodus tangshanensis / Histiodella holodentata	Eoplacognathus pseudoplanus / D. tablepointensis						
462		[?]	Yangtzeplacognathus crassus	Yangtzeplacognathus crassus					
463		Dapingian	Lenodus variabilis	Paroistodus originalis	Paroistodus horridus				
464			L. antarcticus						
465			Microzarkodina parva						
466			Paroisto. originalis						
467			Baltoniodus navis	[?]					
468			Balton. triangularis						
469		Jumudontus ganada	Oepikodus evae	Oepikodus evae	Periodon cf. P. hankensis				
470		469.42	[?]	[?]					
471		471.26							
472	Lower Floian								

Fig. 2. Continued.

reasonable precision in both the relatively shallow-water carbonate facies and the deeper-water graptolite facies. The Dapingian Stage was ratified by the ICS in 2007.

The Darriwilian Stage

The global Darriwilian Stage retains its original concept from the Australasian succession (see Vandenberg and Cooper 1992) spanning the interval from the first appearance of the graptolite *Levisograptus austrodentatus* to the first appearance of *Nemagraptus gracilis*. Unfortunately, no continuous section in Victoria, Australia crossed the lower boundary of the

regional stage (Vandenberg and Cooper 1992) and an appropriate section for the global stage needed to be found elsewhere. The GSSP for the base of the Darriwilian Stage is set at the level of the first appearance of *Levisograptus austrodentatus* at the base of Bed AEP 184, 22 m below the top of the Ningkuo Formation at the Huangnitang section, near Changshan, Zhejiang Province, SE China (Mitchell *et al.* 1997). At the Huangnitang section, the FAD of *L. austrodentatus* occurs within a well-studied succession of graptolite first appearances (including *Levisograptus sinodentatus*, *Arienigraptus zhejiangensis*, *Undulograptus formosus* and *Undulograptus primus*) that occur in a similar

Ordovician biozonation

(e)

Ordovician Biozones						
AGE (Ma)	Conodont Zones					
	Stage	Argentina Precordillera	NW Argentina	Australia (platform)	E. Australia (slope-basinal)	
457	Upper Dariwilian	Baltoniodus variabilis	'Erismodus'	Pygodus anserinus	Pygodus anserinus	Pygodus anserinus
458		Pygodus anserinus				
459		Pygodus serra				
460		Pygodus anitae				
461		Histiodella kristinae				
462		Eoplacognathus suecicus				
463		Microzarkodina ozarkodella				
464		Microzarkodina hagetiana				
465		Yangtzeplacognathus crassus				
466		Lenodus variabilis				
467		Microzarkodina parva				
468		Baltoniodus navis				
469		B. triang./T. laevis				
470	Dapingian	Oe. intermedius	Balton. cf. triang.	Jumudontus ganada	Periodon hankensis	[?]
471		Oepikodus evae				
472	Lower Floian	Trapez. dipron		P. tabellum		[?]

Fig. 2. Continued.

order in many regions around the world. Hence, the level stage boundary can be identified even without the presence of the key taxon. The base of the Darriwilian Stage correlates with the *Aulograptus cucullus* Graptolite Zone in high-latitude successions (Britain).

Limestone interbeds in the Ningkuo Formation at Huangnitang yield diagnostic conodonts (Mitchell *et al.* 1997). Samples from below the GSSP level (beginning with sample AEP 167) contain conodonts that correlate with the *Paroistodus originalis* Zone, and samples from Bed AEP 250, approximately 13 m above the GSSP, contain *Yangtzeplacognathus crassus*. By interpolation, the stage base is close to the base of the *Lenodus*

antivariabilis Conodont Zone, which is defined by the appearance of *L. antivariabilis* and *Baltoniodus norrlandicus* in the Baltoscandian succession. The GSSP correlates with a level slightly above the FAD of the zonal index *Histiodella sinuosa* in the North American (midcontinent) conodont succession (Chen and Bergström 1995). In the Argentine Precordillera and Laurentia, species of the evolving conodont genus *Histiodella* provide a biostratigraphically useful set of biozones that span the lower and middle Darriwilian. From oldest to youngest, these are the *Histiodella sinuosa*, *Histiodella holodentata*, *Histiodella kristinae* and *Histiodella bellburnensis* zones (Stouge 2012; Serra *et al.* 2019) (Fig. 2c, e).

(a)

Ordovician Biozones						
Graptolite Zones						
AGE (Ma)	Stage	Baltica	Britain	South China	Australasia	
443	Silurian					
443.07						
444	Hirnantian	<i>Metabolograptus persculptus</i>	<i>Metabolograptus persculptus</i>	<i>Metabolograptus persculptus</i>	<i>Metabolograptus persculptus</i>	
445		[?]	<i>Metabolograptus extraordinarius</i>	<i>Metabolograptus extraordinarius</i>	<i>Metabolograptus extraordinarius</i>	
445.21						
446						
447						
448						
449	Katian	[?]	<i>Dicellograptus anceps</i>	<i>Paraorthograptus pacificus</i>	<i>Paraorthograptus pacificus</i>	
				<i>Dicellogr. complexus</i>	<i>pre-P. pacificus</i>	
				<i>Dicellogr. complanatus</i>	<i>Dicellogr. complanatus</i>	<i>Alulagraptus uncinatus</i>
				<i>Pleurograptus linearis</i>	<i>Pleurograptus linearis</i>	<i>Dicellograptus elegans/ Orthograptus quadrifurcatus</i>
						<i>Dicellograptus gravis</i>
						<i>Dicranograptus kirki</i>
450						
451						
452						
452.75						
453						
454	Sandbian	<i>Mesograptus foliaceus</i>	<i>Mesograptus foliaceus</i>	<i>Climacograptus bicornis</i>	<i>Climacograptus bicornis</i>	<i>Orthograptus calcaratus</i>
455						
456						
457						
458	458.18	<i>Nemagraptus gracilis</i>	<i>Nemagraptus gracilis</i>	<i>Nemagraptus gracilis</i>	<i>Nemagraptus gracilis</i>	
459	Mid	<i>Jiangxigraptus vagus</i>	<i>Hustedograptus teretiusculus</i>	<i>Jiangxigraptus vagus</i>	<i>Jiangxigraptus vagus</i>	<i>Archiclimacograptus riddellensis</i>

Fig. 3. (a)–(e) Upper Ordovician timescale, stages, and graptolite, conodont and chitinozoan zonal schemes. The leftmost column is the chronometrical timescale from Goldman *et al.* (2020, in Gradstein *et al.* 2020). Zonations and correlations for graptolites are modified from the following (and references therein): Vandenberg and Cooper (1992), Goldman *et al.* (2007a, 2020), Zalasiewicz *et al.* (2009), Cooper and Sadler (2012), Loydell (2012), Maletz and Ahlberg (2018), and Maletz (2021); for conodonts they are modified from Bergström and Wang (1995), Zhen and Percival (2003, 2017), Albanesi and Ortega (2016), Z. H. Wang *et al.* (2019), Zhang *et al.* (2019) and Goldman *et al.* (2020); and for chitinozoans from Paris *et al.* (2004), Nölvak *et al.* (2006) and Goldman *et al.* (2020). ¹The South Gondwana graptolite zonation for the Upper Ordovician is adapted from Gutiérrez-Marco *et al.* (2017).

At the West Bay Centre Quarry, Newfoundland, Canada, a well-dated K-bentonite bed (464.57 ± 0.95 Ma) occurs within the *Holmograptus spinosus* graptolite Zone (Maletz *et al.* 2011; Sell *et al.*

2011). Limestone samples collected around the K-bentonite bed yield *Histiodella* cf. *holodentata* followed by *Histiodella kristinae* higher in the section (upper Table Cove Formation). These data

Ordovician biozonation

(b)

Ordovician Biozones					
Graptolite Zones					
AGE (Ma)	Stage	North America	Argentina Precordillera	NW Argentina	South Gondwana ¹
443	443.07 Silurian				
444			<i>Metabolograptus persculptus</i>		<i>Metabolograptus persculptus</i>
445	Hirnantian		<i>Metabolograptus extraordinarius</i>	<i>Metabolograptus extraordinarius</i>	[?]
445.21					<i>Normalograptus charis</i>
446					[?]
447			<i>Paraorthograptus pacificus</i>	[?]	
448					
449	Katian		<i>Dicellograptus ornatus</i>	<i>Dicellograptus ornatus</i>	<i>Archi-climacograptus vulgatus</i>
450			<i>Dicellograptus complanatus</i>	<i>Dicellograptus complanatus</i>	
451			<i>Syracograptus tubuliferus</i>	<i>Amplexograptus manitobensis</i>	
452			<i>Styacograptus tubuliferus</i>		
452.75					
453					
454					
455	Sandbian		<i>Diplacanthograptus spiniferus</i>		
456					
457			<i>Diplacanthograptus caudatus</i>	<i>Diplacanthograptus caudatus</i>	<i>Archi-climacograptus trubinensis</i>
458					
458.18					
459	Mid	Darriwilian	<i>Climacograptus bicornis</i>	<i>Climacograptus bicornis</i>	[?]
			<i>Nemagraptus gracilis</i>	<i>Nemagraptus gracilis</i>	<i>Orthograptus bekkeri</i>
			<i>Hustedograptus teretiusculus</i>	<i>Hustedograptus teretiusculus</i>	<i>Hustedograptus teretiusculus</i>

Fig. 3. Continued.

provide an important age-dated tie point for Middle Darriwilian graptolite and conodont biostratigraphy (Klebold *et al.* 2019).

Zhen *et al.* (2020b) reported graptolites and conodonts from the Abercrombie Formation of southern New South Wales. The fauna included the graptolites *Isograptus divergens* and *Levisograptus austrodentatus*, along with conodonts identified as *Periodon flabellum* and *Paroistodus* sp. They noted that the specimens of *Periodon flabellum*

represented an advanced morphotype of the species, a morphotype that also occurs in the Cow Head Group of Newfoundland (*Periodon* sp. aff. *P. flabellum* of Stouge 2012). This new report confirms that the range of *P. flabellum* extends into the basal Darriwilian, and facilitates the international correlation of the base of the Darriwilian Stage.

The boundary between the Dapingian and Darriwilian stages marks the decline of the dichograptid and isograptid graptolite clades, and the radiation

(c)

		Ordovician Biozones			
AGE (Ma)		Chitinozoan Zones		Conodont Zones	
		Baltica	North Gondwana	Baltica	N. America Midcontinent
443	443.07 Silurian			<i>Distomodus kentuckyensis</i>	<i>Distomodus kentuckyensis</i>
444	Upper Hirnantian	<i>Conochitina scabra</i>	<i>Spinachitina oulebsiri</i>	<i>Ozarkodina hassi</i>	<i>Ozarkodina hassi</i>
445		<i>Spinachitina taugourdeau</i>	<i>Tanuchitina elongata</i>		<i>Aphelognathus shatzeri</i>
446		<i>Belonechitina gamachiana</i>	<i>Ancyrochitina merga</i>		<i>Aphelognathus divergens</i>
447		<i>Tanuchitina anticostiensis</i>			<i>Aphelognathus grandis</i>
448		<i>Conochitina rugata</i>	<i>Armoricochitina nigerica</i>		<i>Oulodus robustus</i>
449			<i>Acanthochitina barbata</i>		<i>Oulodus velicuspis</i>
450			<i>Tanuchitina fistulosa</i>		<i>Belodina confluens</i>
451		<i>Fungochitina spinifer</i>	<i>Belonechitina robusta</i>		<i>Plectodina tenuis</i>
452			<i>Euconochitina tanvillensis</i>		<i>Phragmodus undatus</i>
453			[?]		<i>Belodina compressa</i>
454		<i>Spinachitina cervicomis</i>			<i>Baltoniodus alobatus</i>
455		<i>Belonechitina hirsuta</i>	<i>Lagenochitina dalbyensis</i>		<i>Erismodus quadridactylus</i>
456		<i>Lagenochitina dalbyensis</i>	<i>Angochitina curvata</i>		<i>Plectodina aculeata</i>
457			<i>Armoricochitina granulifera</i>		<i>Cahabagnathus sweeti</i>
458		<i>Laufeldochitina stenor</i>	<i>Lagenochitina deunffii</i>		
459	Mid Darriwilian		<i>Lagenochitina ponctei</i>		
			<i>Linochitina pissotensis</i>		

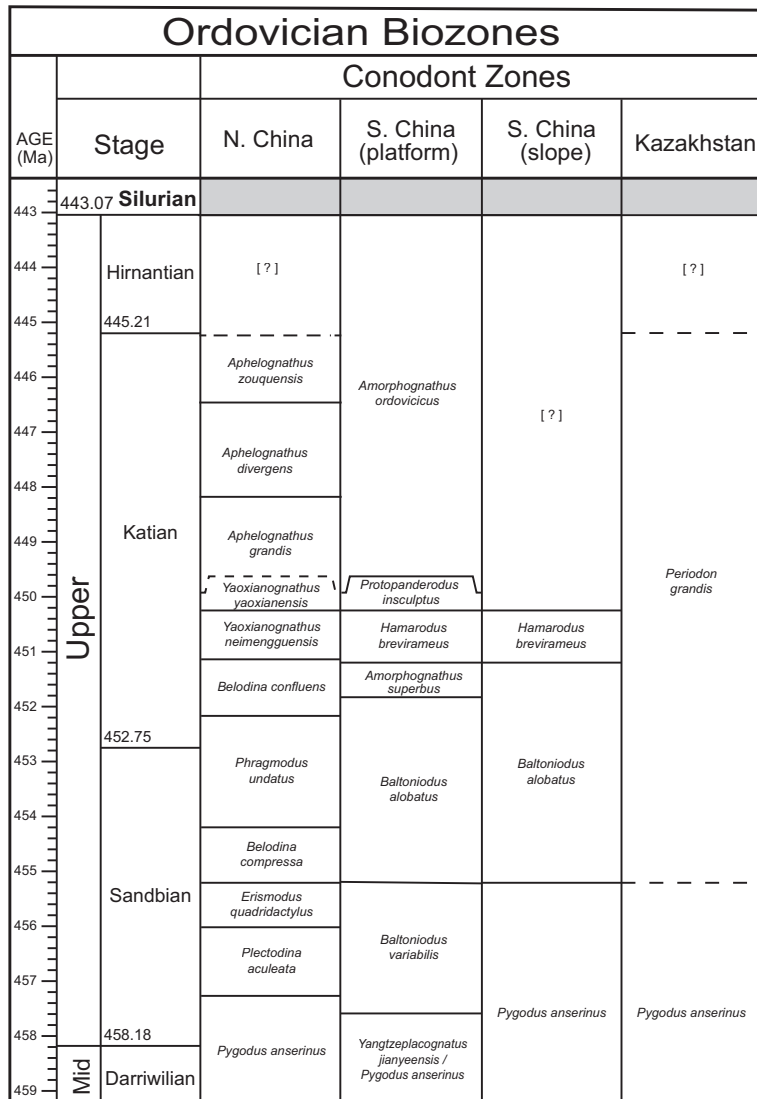
Fig. 3. *Continued.*

of the diplograptids and glossograptids. The rapid evolution and dispersal of the Diplograptacea along with the appearance of several distinctive pseudisograptid and glossograptid species is a globally recognized faunal transition (Mitchell *et al.* 1997; Sadler *et al.* 2011). The appearance and rapid diversification of diplograptids in the lower Darriwilian leads to a high point in Ordovician graptolite species richness. This diversity peak is followed by a decline and then short recovery in the *Archiclimacograptus decoratus* Zone (Da3 of the Australasian succession). The

short-lived Da3 diversity rise is due to a brief, final radiation of dichograptids and glossograptids, including didymograptids, sigmograptids, sinograptids, isograptids and glossograptids (Cooper *et al.* 2004, 2014; Sadler *et al.* 2011). The disappearance of nearly all these taxa (some glossograptids and didymograptids persist into the Sandbian) records a significant extinction event at the end of Da3, an event that precedes the radiation of a distinctive and abundant group of Late Ordovician graptolites, the Dicranograptacea.

Ordovician biozonation

(d)

**Fig. 3.** *Continued.*

The Darriwilian Stage was approved by the ICS in 1997. The level and location of the GSSP in the Huangnitang section are widely accepted and uncontroversial.

The Sandbian Stage

The lowermost stage of the Upper Ordovician Series, the Sandbian Stage, has its GSSP in an outcrop named E14 along the Sularp Brook in the Fågelsång Nature Preserve in the village of Södra Sandby, about 8 km east of the city of Lund in the province

of Scania in southern Sweden. The biostratigraphic level of the base of the Sandbian is the first appearance level of the widespread graptolite *Nemagraptus gracilis* (Fig. 5), which is 1.4 m below the lithologically distinctive Fågelsång Phosphorite, a marker bed in the Almelund Shale known from several localities in Scania (Bergström *et al.* 2000). This biostratigraphic level is coeval with the base of the Caradoc Series in the British succession (Fortey *et al.* 1995), the base of the Chinese Neichanian Stage (Zhang *et al.* 2019) and the base of the Australian Gisbornian Stage (Vandenbergh and Cooper 1992).

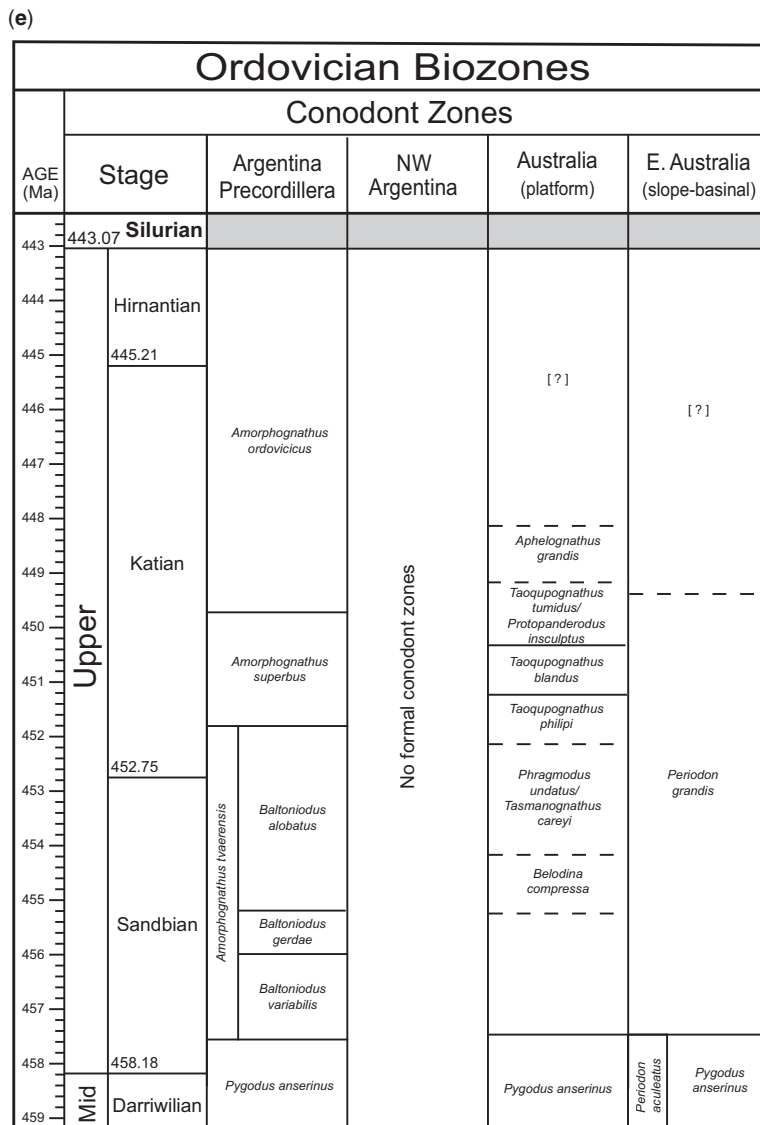


Fig. 3. *Continued.*

In terms of conodont biostratigraphy, this level is at about the middle of the *Pygodus anserinus* Zone and near the base of the *Amorphognathus inaequalis* Subzone. Relative to the Baltic chitinozoan zonation, this level correlates with the base of the *Eisenackithina rhenana* Subzone of the *Laufeldochitina stentor* Zone.

The stage is named after the village of Södra Sandby, the location of the GSSP. The type section was approved by the IGS in 2002 and the stage designation in 2005 ([Nölvak et al. 2006](#)). The greater

part of the Sandbian Stage corresponds to the *Amorphognathus tvaerensis* Conodont Zone. Based on the evolution of the *Baltoniodus* lineage, three subzones are recognized in this conodont zone, namely the *B. variabilis*, *B. gerdæ* and *B. alobatus* subzones (Bergström 1971). These sub-zones have been recognized in many parts of the world and they provide useful long-distance correlations (e.g. Nölvak and Goldman 2007; Goldman *et al.* 2015; Albanesi and Ortega 2016; Chen *et al.* 2017).

Ordovician biozonation



Fig. 4. Photograph of the graptolite *Paratetrograptus approximatus*, index fossil for the base of the Floian Stage. The figured specimen is from Diabasbrottet, Hunnberg. Specimen Cn 1545 Naturhistoriska riksmuseet (Swedish Museum of Natural History), Stockholm, Holm Collection. The photograph was kindly provided by Jörg Maletz. Top-left of scale bar in mm.

It should be noted that based on the graphic correlation of North American and Welsh sections with the Koängen drill core in Scania, Bettley *et al.* (2001) suggested that the FAD of *Nemagraptus gracilis* is younger in the GSSP than at other sites and that there is a gap in the succession at the Fågelsång Phosphorite. However, this latter level is well above the FAD of *N. gracilis* and, hence, does not affect the definition of the stage base at the GSSP. Vandebroucke (2004) noted that two chitinozoan zones (*Angochitina curvata* and *Armoricochitina granulifera*) are missing at the level of the Fågelsång Phosphorite but whether this is due to a stratigraphic gap or if the time represented by these zones is contained within the apparently slowly deposited phosphorite bed remains unknown. Further work using



Fig. 5. Photograph of the graptolite *Nemagraptus gracilis*, index fossil for the base of the Sandbian Stage and Upper Ordovician Series. The figured specimen was collected from the Mount Merino Shale (Normanskill) near Albany, NY. Specimen AMNH 36766, the American Museum of Natural History, New York City. Originally figured by Hall (1859, p. 512, fig. 6). Scale bar at bottom in mm.

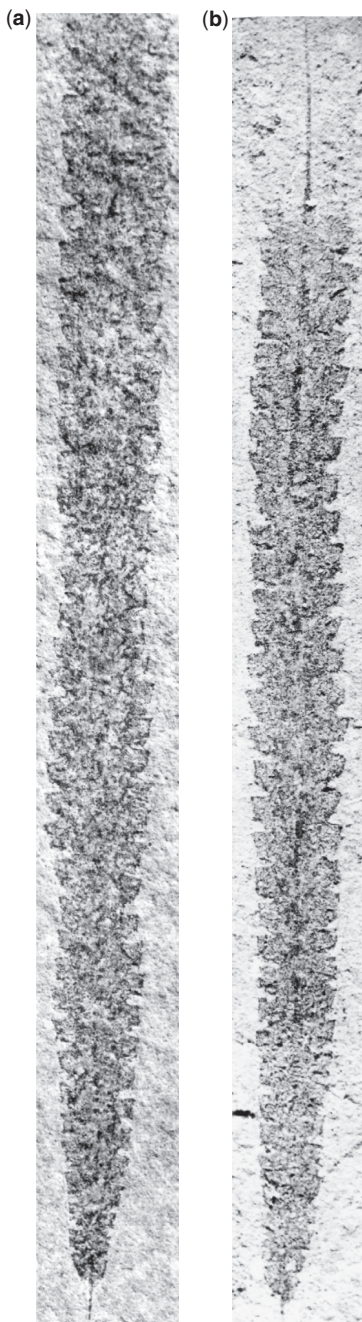


Fig. 6. Photographs of the graptolite *Metabolograptus extraordinarius*, index fossil for the base of the Hirnantian Stage. The figured specimens are from the Honghuayuan section, Tongzi, China: (a) specimen NIGP133403, also figured in Chen *et al.* (2005, pl. 1, fig. 1); and (b) specimen NIGP133400, also figured in Chen *et al.* (2005, pl. 1, fig. 2). Both specimens X4.5. The photographs were kindly provided by Chen Xu and Chen Qing.

quantitative correlation and multiple fossil groups is needed to resolve these issues.

The Katian Stage

The base of Katian Stage is one of the most tightly constrained levels in the Ordovician timescale (Goldman *et al.* 2020). The GSSP for the base of the Katian Stage is set at the level of the first appearance of the morphologically distinctive and globally distributed graptolite *Diplacanthograptus caudatus* at a quarried exposure along Black Knob Ridge, about 5 km NE of Atoka in southeastern Oklahoma, USA (Goldman *et al.* 2007a). The level is 4.0 m above the base of the Bigfork Chert.

The FAD of *Diplacanthograptus caudatus* is very close to the first appearances of several other widespread graptolite species, including *Diplacanthograptus lanceolatus*, *Corynoides americanus*, *Orthograptus pageanus*, *Orthograptus quadrimumcronatus*, *Dicranograptus hians* and *Neurograptus marginatus*. The base of the Katian Stage is also close to the first appearance of the zonal index graptolite *Dicranograptus clingani*, a species common in middle- to high-palaeolatitude locations.

At Black Knob Ridge, two K-bentonites occur in the upper Womble Shale (*Climacograptus bicornis* Zone) at 5.5 and 6.6 m below the Katian GSSP level. These beds were dated by Sell *et al.* (2013) and yielded ages of $453.98 \pm 0.33/0.38/0.62$ and $453.16 \pm 0.24/0.31/0.57$ Ma, respectively. In the Mohawk River Valley of New York State, USA, MacDonald *et al.* (2017) calculated exceptionally precise dates for two K-bentonites that occur low in the *Diplacanthograptus caudatus* Zone. These K-bentonites yielded dates of 452.63 ± 0.06 and 451.71 ± 0.13 Ma, respectively. By interpolation, the base of the Katian Stage is estimated to be 452.75 ± 0.7 Ma in age (Goldman *et al.* 2020).

With respect to conodont biostratigraphy, the base of the Katian Stage occurs in the upper part of the North Atlantic conodont zone of *A. tvaerensis*, just below the base of the *Plectodina tenuis* Zone and in the middle–upper part of the chitinozoan *Spi-nachitina cervicornis* Zone (approximately coincident with the base of the *Angochitina multiplex* Subzone).

The base of the Katian Stage is also constrained by other important marker horizons. The Millbrig and Kinnekulle K-bentonite complexes in eastern North America and Scandinavia, respectively, lie just below the GSSP level, as does the beginning of the positive $\delta^{13}\text{C}$ Guttenberg isotopic carbon excursion (GICE).

Graptolite biodiversity fluctuates sharply during the Katian (Cooper *et al.* 2014). In the lowermost part of the Katian, perhaps in response to global climate perturbations (Goldman and Wu 2010; Pohl

et al. 2016), graptolite faunas exhibit a distinct decline in both morphological and taxonomic diversity (Goldman and Wu 2010). This post-Sandbian decline is followed by a brief diversity rebound, and then another decline in the middle Katian. The upper part of the Katian Stage contains a species diversity peak, driven by a diversification of the diconograptid–climacograptid–orthograptid (DCO) graptolite fauna (Chen *et al.* 2005).

The end of the Katian Stage (and beginning of the overlying Hirnantian Stage) is marked by the most severe decline in graptolite diversity within the entire Ordovician, during which the DCO fauna, along with a wide range of other fossil groups, became extinct (Melchin and Mitchell 1991; Chen *et al.* 2005; Finney *et al.* 2007). Global conodont diversity is low in the early Katian, rises in the middle Katian but stays well below their peak Middle Ordovician levels (Sweet 1988).

The name ‘Katian’ is taken from Katy Lake (now drained) near the southern end of Black Knob Ridge (Bergström *et al.* 2006). The ICS ratified the GSSP and the stage name in 2005.

The Hirnantian Stage

The GSSP for the uppermost stage of the Ordovician, the Hirnantian Stage, is placed at the stratigraphic level of the first appearance of the graptolite *Metabolograptus extraordinarius* (Fig. 6) at the Wangjiawan North section, 0.39 m below the base of the Kuanyinchiao Bed, 42 km north of Yichang city, western Hubei, China (Chen *et al.* 2006). The stage is named after the Hirnant Limestone at Bala in Wales and closely matches the classical Hirnantian, the uppermost subdivision of the Ashgill Regional Series of Britain.

The Hirnantian Stage records a remarkable interval in Earth history. It spans an interval of major climatic and eustatic changes, and one or more strong positive carbon isotope excursions, which are events associated with the end-Ordovician glaciation (Brenchley *et al.* 2003; Melchin *et al.* 2013). The first of the Phanerozoic’s five great extinction events, the Late Ordovician mass extinction (LOME), ostensibly driven by global climate change and associated sea-level fluctuations, produced a dramatic decline in the diversity of the Earth’s marine biota, including graptolites (e.g. Harper *et al.* 2014; Crampton *et al.* 2018). The LOME is most severe in the *M. extraordinarius* and *Metabolograptus persculptus* graptolite zones, although some diversity decline began in the latest Katian.

A distinctive shelly fossil association, the *Hirnantia–Dalmanitina* fauna (commonly referred to as the ‘Hirnantia fauna’), is globally distributed in strata of latest Ordovician (generally Hirnantian) age (Rong and Harper 1988). There is some

Ordovician biozonation

published disagreement regarding the correlation of the graptolite-defined Hirnantian GSSP into carbonate facies sections, particularly its correlation with the Baltic chitinozoan zonation (cf. Holmden *et al.* 2013; Bergström *et al.* 2014). However, recent work from Baltoscandia and Anticosti Island place the boundary in the *Belonechitina gamachiana* Chitinozoan Zone (Melchin 2008; Mauviel and Desrochers 2016; Amberg *et al.* 2017).

The stratigraphic level of first appearance of the graptolite *Akidograptus ascensus* in the Dob's Linn section of southern Scotland defines the base of the Silurian System and the top of the Hirnantian Stage (Melchin *et al.* 2012, 2020).

Ordovician biozones

Regional zonations and their correlation with Ordovician chronostratigraphic units and ages are shown in Figures 1a–e (Lower Ordovician zones), 2a–e (Middle Ordovician zones) and 3a–e (Upper Ordovician zones).

Graptolite zones

Graptolite faunas exhibited strong biogeographical differentiation during the Ordovician, a fact reflected in the abundance of regional zonations. Skevington (1973, 1974) recognized two major graptolite faunal provinces: the mid- to high-palaeolatitude ‘Atlantic Province’ and the low-palaeolatitude ‘Pacific Province’; but these have been shown to be overly general and simplistic, particularly because the controls on faunal provincialism are numerous and complex (see Goldman *et al.* 2013 and references therein for a comprehensive review of graptolite biogeography). Nevertheless, graptolite zonations, which have been erected from multiple regions around the world (Loydell 2012; Maletz 2021), tend to fall into low- and high-latitude groups. In low-latitude environs (‘Pacific Province’, 30° N–30° S), the Australasian zonal scheme spans almost the entire Ordovician and is one of the most finely subdivided and useful regional frameworks (Figs 1a, 2a & 3a) (Harris and Thomas 1938; Thomas 1960; Vandenberg and Cooper 1992). It comprises 30 zones, two of which are split into subzones, with an average duration of 1.5 myr each. The Australasian graptolite succession is, however, incomplete in the Tremadocian (Maletz and Ahlberg 2011; Maletz 2021).

The Australasian zonation is widely applicable in most Pacific Province graptolite successions but faunal endemism in some regions and intervals required the construction and use of local zonations, which may better fit the local succession and provide a finer resolution for correlation (e.g. the endemic

lower–middle Katian zonation from the Appalachian Basin of eastern North America).

The classic zonal scheme for middle–high palaeolatitudes (Atlantic Province) is that of England and Wales (Zalasiewicz *et al.* 2009) (Figs 1a, 2a & 3a) where some 17 zones span the Tremadoc–Ashgill (Tremadocian–Hirnantian global stages), averaging 2.3 myr each. The focus on defining global series and stages for the Ordovician has had an interesting but unfortunate effect on our understanding of high-palaeolatitude biostratigraphy and biodiversity. In an attempt to define globally recognizable biozones, graptolite workers concentrated on finding cosmopolitan species that would be useful in inter-regional correlations. Endemic taxa were sometimes misidentified, ignored or shoehorned into better-known tropical species (e.g. see Goldman *et al.* 2013; Kraft *et al.* 2015).

Recent work on the taxonomy and biostratigraphy of central European graptolite faunas (Kraft *et al.* 2015; Gutiérrez-Marco *et al.* 2017), however, has helped to refine a peri-Gondwanan graptolite zonation. Similarly, new detailed work by Toro *et al.* (2015), Toro and Maletz (2018), Herrera Sánchez *et al.* (2019) and Toro and Herrera Sánchez (2019), to cite just a few, has greatly improved the global correlations of Tremadocian–mid-Dapingian strata in the Central Andean Basin. Although many species were cosmopolitan and correlation between low- and high-palaeolatitude regions is fairly well constrained throughout most of the period, understanding high-palaeolatitude biodiversity and correlating regional zonal schemes with global series and stages remains a work in progress (Gutiérrez-Marco and Martin 2016; Gutiérrez-Marco *et al.* 2017; Herrera Sánchez and Toro 2022). For a short summary of the history of graptolite biostratigraphy, the reader is directed to Maletz (2021).

Conodont zones

Ordovician conodont faunas are distributed in two major biogeographical realms: a Shallow-Sea Realm (SSR) and an Open-Sea Realm (OSR) (Zhen and Percival 2003). Sweet and Bergström (1976, p. 123; 1984, p. 70) described a ‘warm-water North American Midcontinent Province’ that ranged about 30 degrees N and S of the Equator, and a ‘cool-water North Atlantic Province’ that extended polewards from 30 to 40 degrees latitudes. Zhen and Percival (2003) recognized that the North American midcontinent region of Sweet and Bergström (1976) was one of up to seven provinces in what they defined as the SSR, and what Sweet and Bergström (1976, 1984) described as the North Atlantic Province encompasses both the OSR and the Temperate and Cold Domains of the SSR. Carbonate facies and associated rocks from these two realms

D. Goldman *et al.*

contain diverse and rich faunas that can be finely zoned into 26 zones, some of which are further divided into subzones (Figs 1b, 2b & 3b). It is important to note that the zones of the North American midcontinent region (Laurentian Province of Zhen and Percival 2003) were initially based on traditional biostratigraphic zonal practices (Sweet and Bergström 1976 and references therein). Sweet (1984, 1995) used graphic correlation to construct and formally name midcontinent conodont chonozones, using many of the same taxon names that were used for the biostratigraphic zones. Sweet (1988) provided a useful range charts for many taxa in his conodont chonozonation but refers to them as conodont-defined biozones, and they are generally based on the first appearance of the biozone name-bearing taxon. This changing of definitions between graphic correlation-defined chonozones to biozones, together with the apparent control of many Laurentian conodont species ranges by local habitat conditions related to water depth, has led to conflicting or misleading correlations. The Cold Domain of Zhen and Percival (2003) is best known from the Baltic region in which 17 zones and several subzones are recognized. Zonations derived from faunas in North and South China (Zhang *et al.* 2019; Z.H. Wang *et al.* 2019), the Argentine Precordillera and NW Argentina (Albanesi and Ortega 2016), Australia (Zhen and Nicoll 2009; Zhen *et al.* 2015, 2020a; Zhen and Percival 2017), and Kazakhstan (Tolmacheva *et al.* 2021) have added substantially to our understanding of conodont provincialism and biostratigraphy. These regional zonations are correlated with the GTS 2020 Carbonate Facies biozones of Goldman *et al.* (2020) in Figures 1, 2 and 3 but additional work to establish precise zonal ties is required.

Chitinozoan zones

Chitinozoans are widely occurring marine microfossils that have proved to be very useful index fossils in the Middle and Upper Ordovician. They are less diverse in the Lower Ordovician (Paris *et al.* 2004). Chitinozoans are currently best known from northern Gondwana (e.g. Paris 1990) where 25 zones have been recognized in the Ordovician. A significant amount of work has also been conducted in the Ordovician of Baltoscandia where 18 zones and 10 subzones have been distinguished (e.g. Nölvak *et al.* 2006). Less work has been carried out on this group in North America where chitinozoans currently remain unstudied in large regions. Exceptions to this include the Middle and Upper Ordovician faunas of Anticosti Island in eastern Canada (e.g. Achab 1989). The diverse chitinozoan faunas of the Upper Ordovician of the North America Midcontinent have been the subject of some study (e.g. Jenkins

1969; Liang *et al.* 2019, 2020) but those of the Lower Ordovician of that vast region remain virtually unknown. In recent years, the Ordovician chitinozoans of the Yangtze Platform in China have been investigated by several workers (e.g. Chen *et al.* 2009; Liang and Tang 2016; Liang *et al.* 2018; W.H. Wang *et al.* 2019). The successions of Baltoscandic and Gondwana chitinozoan zones are illustrated in Figures 1c, 2c and 3c.

Integration of graptolite, conodont and chitinozoan zones

On a global scale, Ordovician rocks show a striking latitudinal differentiation in biofacies. This probably reflects the influence of climatic belts and depositional depth. For instance, the low-latitude tropical faunas of the North American Midcontinent have very little in common with coeval faunas of Baltoscandia, which inhabited more high-latitude, temperate environments. There is also a striking difference between the shallow-water and deep-water faunas in these regions. These differences in biofacies cause long-range biostratigraphic correlation problems that may be difficult, or impossible, to solve using a single fossil group. One way to clarify the relations between different biofacies is to use co-occurrences of fossils that tend to occur in different biofacies, such as stratigraphic intervals in which biostratigraphically important conodonts co-occur with graptolites. Conodonts may be preserved on shale surfaces in graptolite shales, as is the case at the Sandbian GSSP in southern Sweden (Bergström *et al.* 2000; Bergström 2007) and at the Katian GSSP at Black Knob Ridge, Oklahoma, USA (Goldman *et al.* 2007a). Unfortunately, such co-occurrences are not very common.

More common are conodonts that occur in carbonate-rich intervals in graptolite shales. Examples of such important occurrences include the Darriwilian–Sandbian Athens Shale of Alabama (Finney 1977), the Cow Head Group of western Newfoundland (Cooper *et al.* 2001; Stouge 2012), the Dawangou Section in the Tarim region of northwestern China (Chen *et al.* 2006, 2017), the Viola Group of Oklahoma (Finney 1986), Darriwilian–Sandbian limestones in Sweden (Jaanusson 1960) and the Kandava drill core of Latvia (Goldman *et al.* 2015).

In an attempt to clarify the relations between conodont and graptolite donations globally, Bergström (1986) reviewed the literature and found 78 direct ties between the fossil zonations. In a later study, Bergström *et al.* (in Chen *et al.* 2017) presented 27 additional tie points, reaching a total of 105 graptolite–conodont zonal ties.

Chitinozoans are commonly present in both shales and limestones within graptolite shale

Ordovician biozonation

successions. In such cases it is possible to isolate chitinozoans from the shales using strong acids that can dissolve clastics (e.g. Vandenberg 2004, 2008a, b; Goldman *et al.* 2007a, b; Leslie *et al.* 2008; Vandenberg 2013).

In a few regions of the world, there is a series of juxtaposed biofacies/lithofacies belts that range from shallow to deep water. Perhaps the best known such region is Baltoscandia, where Jaanusson (1976, 1995) recognized a series of such belts. He referred to these as confacies belts. These confacies belts – the Scanian (slope; black shale), Central Baltoscandian (outer shelf; argillaceous limestones) and North Estonian (carbonate platform) belts – record an offshore to onshore transition along the eastern to southeastern margin of the East European Craton. In terms of water depth, the shallowest is the North Estonian confacies belt, which represents a shallow-water carbonate platform. Somewhat deeper depositional environments are represented by the central Baltoscandian confacies belt, which represents the outer shelf and is characterized by more or less argillaceous limestones. The deepest-water deposits are found in the Scanian confacies belt where dark shales dominate. The densely sampled outcrops and drill cores across this region, which commonly exhibit interfingering lithofacies at the confacies belt transitional areas, have facilitated detailed zonal ties between graptolites, conodonts and chitinozoans (e.g. Goldman *et al.* 2015). Comprehensive searches for fossil occurrences outside their common biofacies association, detailed sampling of regions that have onshore–offshore transects and the use of quantitative stratigraphic methods to interleave datasets have further advanced the integration of graptolite, conodont and chitinozoan zones (Goldman *et al.* 2020).

Outcrops that provide perhaps the most valuable data for precise global correlations and timescale construction contain stratigraphic range data from two or more clades, as well as radioisotope dated K-bentonite beds. Examples of these localities include the mid-Darriwilian West Bay Centre Quarry in Newfoundland (graptolite and conodont biostratigraphy with a dated K-bentonite: see Maletz *et al.* 2011; Sell *et al.* 2013; Klebold *et al.* 2019) and the Black Knob Ridge section in Oklahoma, USA (Katian GSSP, graptolite and conodont biostratigraphy with a dated K-bentonite: see Goldman *et al.* 2007a, b; Sell *et al.* 2013).

Chemostratigraphy, and especially that based on $\delta^{13}\text{C}$, has become of major importance in Ordovician stratigraphy over the last two–three decades. This technique has been of great significance in resolving many stratigraphic relationships that were problematic for conventional biostratigraphy. Chemostratigraphy must, however, be closely integrated with biostratigraphy in order to achieve its greatest utility.

Such detailed integration is an ongoing process. Bergström *et al.* (2009) provided a general summary of the relationship between the major Ordovician isotopic excursions and important chronostratigraphic subdivisions.

In a recent global summary paper, Bergström *et al.* (2020) reviewed the relationships between 15 major $\delta^{13}\text{C}$ excursions and Ordovician graptolite and conodont zones. Although focused on North America, Baltoscandia and Argentina, each of the major carbon isotope excursions are discussed in terms of their presence in both local and global biostratigraphic frameworks, particularly graptolite and conodont zonations. Hence, Bergström *et al.* (2020) describes the biostratigraphic position and duration of four major $\delta^{13}\text{C}$ excursions in the Lower Ordovician, two in the Middle Ordovician and nine in the Upper Ordovician. A full discussion of the importance of Ordovician chemostratigraphy is well beyond the scope of this chapter but, in addition to the summaries cited above, the subject is extensively dealt with elsewhere in this Special Publication.

Quantitative biostratigraphy

The construction of useful biozonations and precise correlation frameworks commonly require the evaluation of large numbers of taxon ranges from multiple stratigraphic sections. In addition, the data may be mined from the published work of many different authors. Hence, these large datasets can have inherent biases such as sampling inconsistencies, range truncations, missing taxa and taxonomic misidentifications. Quantitative biostratigraphic techniques were developed to help manage large datasets, and to more effectively recognize and overcome human and palaeontological biases (Shaw 1964; Miller 1977; Edwards 1995; Kemple *et al.* 1995; Sadler and Cooper 2003; Sadler 2020 among many others). A short review of the graphic correlation and quantitative biostratigraphic technique used in the construction of the 2020 Ordovician timescale (CONOP9) is provided below.

Stratigraphic correlation requires three separate tasks: (1) establishing a temporal sequence of events; (2) determining the relative interval length between those events; and (3) locating the horizons that match in age with each event in every section (Kemple *et al.* 1995). Unfortunately, due to uneven sampling, partial preservation of taxon ranges and missing taxa, the sequence of events (primarily taxon FADs and last appearance datums (LADs)) is often inconsistent between stratigraphic sections (Sadler *et al.* 2009). Traditional graphic correlation (Shaw 1964) solves this problem by plotting the levels of stratigraphic data that two sections have in common on an X–Y biplot. The line of correlation

D. Goldman *et al.*

(LOC) between these two sections represents a proposed solution, which is typically constrained not to allow range contractions in either section, and to require a monotonic relationship between time and rock thickness in each section (Miller 1977; Edwards 1995). The best solution to the correlation problem is the one where the LOC requires the minimum net range extension necessary to make all local ranges match a single sequence and spacing of events. This is called ‘economy of fit’ (Shaw 1964), and, as well as defining a best solution, it can be used to examine levels of ‘misfit’ and define a penalty function that can rank alternate solutions (Kemple *et al.* 1995).

Unlike graphic correlation, which adds data to a composite one section at a time, constrained optimization (CONOP9: Sadler and Cooper 2003) is multi-dimensional – it works with observations from ‘*n*’ numbers of sections simultaneously. CONOP9 proposes sequences of FADs and LADs, rejects impossible solutions (enforcing a constraint), and then searches for the best possible solution (optimization) by searching through many possible solutions using a numerical method called simulated annealing (Kemple *et al.* 1995). The best correlation solutions are those that require the minimum net adjustment of observed ranges in local sections.

Thus, a penalty function based on the sum of range extension for all taxa in all sections can be calculated and used to rank the various possible solutions. Computer software (Sadler 2003) is used to generate large numbers of possible solutions and search for the one with the minimum possible penalty. In sum, CONOP9 eliminates impossible correlation solutions, those that contain last before first appearance datums for any individual species; minimizes unobserved taxon co-existence; and chooses the ‘best’ among the possible solutions – the one that has the minimum net adjustment of observed ranges in local sections and smallest number of unobserved taxon co-existence.

As with all quantitative correlation techniques, composite taxon ranges and correlation models generated in CONOP9 must be carefully examined for inaccuracies, and conflicts with expert observation and opinion should be thoroughly evaluated. Seemingly out of place taxon range ends or unusual species coexistences can have several possible explanations. The most common problem with CONOP9 taxon range charts is taxonomic misidentification. If a species occurrence is misidentified in any input section, its stratigraphic range in the composite could be greatly extended. In traditional biostratigraphy, these outliers can be ignored but CONOP9 accepts the erroneous occurrence as valid. Species ranges that are extended from misidentification can also create unobserved co-existences, which complicates the task of constructing

a workable zonation from the composite range chart. Conversely, CONOP9 makes the recognition of taxa that are out of place in time and space easy to find, and an investigation into possible misidentifications can be carried out. Taxon range ends and section tops or bottoms can also float or sink well beyond any reasonable age assignment for other reasons. Generally, this occurs when there is no constraint on a range or section end. For example, the last collection in a section may contain a single taxon LAD that is artificially truncated at the section top. With no other constraint, CONOP may let the section top float upwards to the actual LAD of that taxon (as it occurs in another section). Finally, of course, unusual taxon ranges may really reflect a better range estimation than can be determined with traditional biostratigraphy.

The current Ordovician and Silurian timescales (Goldman *et al.* 2020; Melchin *et al.* 2020) employ constrained optimization (CONOP9: Sadler 2003; Sadler *et al.* 2009) to construct a composite graptolite range chart (837 stratigraphic sections, 2651 species, and 5302 FADs and LADs) into which radioisotope dates are interpolated.

The stratigraphic ranges of taxa in a composite range chart that is compiled from hundreds of global sections are generally different from those ranges observed at any local section. In addition, the various algorithms used to sequence and space the taxon range ends can themselves produce different taxon ranges and range relationships. Hence, picking bio-zones and stage boundaries in a CONOP9 composite section requires careful consideration and can be accomplished in a variety of ways (Sadler *et al.* 2011; Goldman *et al.* 2020; Sadler 2020).

First, the GSSP level itself, which is entered into the CONOP database as a single occurrence in the stratotype section, can be picked as the stage base. However, as a single section, single event, the GSSP level is not necessarily well constrained in the composite sequence. This means that the CONOP9 algorithm may move the single event to different positions without incurring substantial additional penalty. Second, biozone and stage bases may be located based on the first appearance in the composite sequence of the taxon that defines the GSSP level. This is not always the same level in the composite section as the GSSP level. In addition, in CONOP the placement of all the local first appearances of a zonal index taxon as projected into the composite can be displayed. This provides a means to find outliers (Sadler 2020).

Finally, many biostratigraphic studies with published range charts include their authors’ best estimates of the position of stage boundaries. Sometimes the boundary position is inferred from the taxon ranges of species other than graptolites, conodonts or chitinozoans. These local stage

Ordovician biozonation

boundary approximations were included in the CONOP9 compositing process as very conservative minimum–maximum uncertainty intervals (Goldman *et al.* 2020; Sadler 2020). Hence, one could choose the midpoint, for example, of one of these uncertainty intervals.

In most cases, the GSSP level and the FAD of the species that defines it are very close to one another and within the minimum–maximum uncertainty interval in the CONOP9 composite range chart used for the Ordovician timescale in GTS 2020. However, it is important to note that the enormous benefit of quantitative biostratigraphy in examining and removing biases in the empirical data also generates uncertainties that must be taken into consideration by experts (Sadler *et al.* 2011; Sadler 2020).

On regional scales, Goldman *et al.* (2012, 2013) used CONOP methodology to construct a fully integrated multiclad range chart (graptolites, conodonts, chitinozoans and ostracods) from Middle and Upper Ordovician strata in outcrops and drill cores that spanned all three confacies belts in Baltoscandia. Bryan *et al.* (2018) and Serra *et al.* (2019) also used quantitative correlation to integrate conodont and graptolite biostratigraphy in the Argentine Precordillera, and Herrera Sánchez and Toro (2022) used CONOP9 to establish a correlation model for the Lower and Middle Ordovician of the Central Andean Basin.

Quantitative biostratigraphy is a powerful tool for resolving taxon range inconsistencies between sections and for choosing between multiple possible correlation models. Quantitative methods, which may examine many thousands of reasonable event sequences, can also provide various options to estimate confidence intervals on boundary placements (Sadler 2020). Finally, we have also found that utilizing these methods forces us to examine our datasets critically, which helps uncover and correct many errors in the original literature data, in operator input and in the processing of the data.

Acknowledgements We would like to thank Jörg Maletz and two anonymous reviewers for their helpful comments and careful critique of the manuscript. We also thank John Repetski and Yong-Yi Zhen for reviewing parts of the correlation charts.

Competing interests The authors declare that they have no known competing financial interests or personal relationships that could have appeared to influence the work reported in this paper.

Author contributions DG: formal analysis (equal), methodology (equal), writing – original draft (lead), writing – review & editing (lead); SAL: formal analysis (equal), methodology (equal), writing – original draft (supporting),

writing – review & editing (supporting); YL: formal analysis (equal), writing – original draft (supporting), writing – review & editing (supporting); SMB: formal analysis (equal), writing – original draft (supporting), writing – review & editing (supporting).

Funding This research received no specific grant from any funding agency in the public, commercial, or not-for-profit sectors.

Data availability Data sharing is not applicable to this article as no datasets were generated or analysed during the current study.

Correction notice The copyright has been updated to Open Access.

References

- Achab, A. 1980. Chitinozoaires de l’Arenig inférieur de la Formation de Lévis (Québec, Canada). *Review of Palaeobotany and Palynology*, **31**, 219–239, [https://doi.org/10.1016/0034-6667\(80\)90028-7](https://doi.org/10.1016/0034-6667(80)90028-7)
- Achab, A. 1989. Ordovician chitinozoan zonation of Quebec and western Newfoundland. *Journal of Paleontology*, **63**, 14–24, <https://doi.org/10.1017/S002233600040907>
- Achab, A. and Maletz, J. 2022. The age of the *Euconochitina symmetrica* Zone and implication for Lower Ordovician chitinozoan and graptolite zonations of Laurentia. *Review of Palaeobotany and Palynology*, **295**, 104508, <https://doi.org/10.1016/j.repalbo.2021.104508>
- Albanesi, G.L. and Ortega, G. 2016. Conodont and graptolite biostratigraphy of the Ordovician System of Argentina. In: Montenari, M. (ed.) *Stratigraphy and Timescales. Volume 1*. Academic Press, Cambridge, MA, 61–121, <https://doi.org/10.1016/bs.sats.2016.10.002>
- Aldridge, R.J., Briggs, D.E.G., Smith, M.P., Clarkson, E.N.K. and Clark, N.D.L. 1993. The anatomy of conodonts. *Philosophical Transactions of the Royal Society of London B: Biological Sciences*, **340**, 405–442, <https://doi.org/10.1098/rstb.1993.0082>
- Aldridge, R.J., Murdock, D.J.E., Gabbott, S.E. and Theron, J.N. 2013. A 17-element conodont apparatus from the Soom Shale Lagerstätte (Upper Ordovician), South Africa. *Palaeontology*, **36**, 261–276, <https://doi.org/10.1111/j.1475-4983.2012.01194.x>
- Amberg, C.E.A., Vandenbroucke, T.R.A., Nielsen, A.T., Munnecke, A. and McLaughlin, P.I. 2017. Chitinozoan biostratigraphy and carbon isotope stratigraphy from the Upper Ordovician Skogerholmen Formation in the Oslo Region. A new perspective for the Hirnantian lower boundary in Baltica. *Review of Palaeobotany and Palynology*, **246**, 109–119, <https://doi.org/10.1016/j.repalbo.2017.06.008>
- Bergström, S.M. 1971. Conodont biostratigraphy of the Middle and Upper Ordovician of Europe and eastern North America. *Geological Society of America*

D. Goldman *et al.*

- Memoirs*, **127**, 83–157, <https://doi.org/10.1130/ME-M127-p83>
- Bergström, S.M. 1986. Biostratigraphic integration of Ordovician graptolite and conodont zones – a regional review. In: Rickards, R.B. and Hughes, C.P. (eds) *Paleobiology and Biostratigraphy of Graptolites*. Blackwell Scientific, Oxford, UK, 61–78.
- Bergström, S.M. 2007. Middle and Upper Ordovician conodonts from the Fågelsång GSSP, Scania, southern Sweden. *GFF*, **129**, 77–82, <https://doi.org/10.1080/11035890701292077>
- Bergström, S.M. and Wang, Z.H. 1995. Global correlation of Castlemarian to Darriwilian conodont faunas and their relations to the graptolite zone succession: *Palaeoworld*, **10**, 92–98, <https://doi.org/10.18814/epiugs/2000/v23i2/003>
- Bergström, S.M., Finney, S.C., Chen, X., Palsson, C., Wang, Z.H. and Grahn, Y. 2000. A proposed global boundary stratotype for the base of the Upper Series of the Ordovician System: The Fågelsång section, Scania, southern Sweden. *Episodes*, **23**, 102–109, <https://doi.org/10.18814/epiugs/2000/v23i2/003>
- Bergström, S.M., Löfgren, A. and Maletz, J. 2004. The GSSP of the second (upper) stage of the Lower Ordovician Series: Diabasbrottet at Hunneberg, Province of Västergötland, southwest Sweden. *Episodes*, **27**, 265–272, <https://doi.org/10.18814/epiugs/2004/v27i4/005>
- Bergström, S.M., Finney, S.M., Chen, X., Goldman, D. and Leslie, S.A. 2006. Three new Ordovician global stage names. *Lethaia*, **39**, 287–288, <https://doi.org/10.1080/00241160600847439>
- Bergström, S.M., Chen, X., Guteirrez-Marco, J.-C. and Dronov, A. 2009. The new chronostratigraphic classification of the Ordovician System and its relations to major regional series and stages and to $\delta^{13}\text{C}$ chemostratigraphy. *Lethaia*, **42**, 97–107, <https://doi.org/10.1111/j.1502-3931.2008.00136.x>
- Bergström, S.M., Eriksson, M.E., Young, S.A., Ahlberg, P. and Schmitz, B. 2014. Hirnantian (latest Ordovician) $\delta^{13}\text{C}$ chemostratigraphy in southern Sweden and globally: a refined integration with the graptolite and conodont zone successions. *GFF*, **136**, 355–386, <https://doi.org/10.1080/11035897.2013.851734>
- Bergström, S.M., Schmitz, B., Terfelt, B., Eriksson, M.E. and Ahlberg, P. 2019. The $\delta^{13}\text{C}$ chemostratigraphy of Ordovician global stage stratotypes: geochemical data from the Floian and Sandbian GSSPs in Sweden. *GFF*, **142**, 23–32, <https://doi.org/10.1080/11035897.2019.1631883>
- Bergström, S.M., Eriksson, M.E. and Ahlberg, P. 2020. Ordovician $\delta^{13}\text{C}$ chemostratigraphy: A global review of major excursions and their ties to graptolite and conodont biostratigraphy. In: Montenari, M. (ed.) *Stratigraphy and Timescales. Volume 5*. Academic Press, Cambridge, MA, 319–351, <https://doi.org/10.1016/bs.sats.2020.09.001>
- Bettley, R.M., Fortey, R.A. and Siveter, D.J. 2001. High-resolution correlation of Anglo-Welsh Middle to Upper Ordovician sequences and its relevance to international chronostratigraphy. *Journal of the Geological Society, London*, **158**, 937–952, <https://doi.org/10.1144/0016-764900-193>
- Bockelie, T.G. 1981. Internal morphology of two species of Lagenochitina (Chitinozoa). *Review of Palaeobotany and Palynology*, **34**, 149–164, [https://doi.org/10.1016/0034-6667\(81\)90035-X](https://doi.org/10.1016/0034-6667(81)90035-X)
- Brenchley, P.J., Carden, G.A. *et al.* 2003. High-resolution stable isotope stratigraphy of Upper Ordovician sequences: Constraints on the timing of bioevents and environmental changes associated with mass extinction and glaciation. *Bulletin of the Geological Society of America*, **115**, 89–104, [https://doi.org/10.1130/0016-7606\(2003\)115<0089:HRSISO>2.0.CO;2](https://doi.org/10.1130/0016-7606(2003)115<0089:HRSISO>2.0.CO;2)
- Bryan, A., Goldman, D., Albanesi, G.L., Ortega, G. and Serra, F. 2018. Computer-assisted graphic correlation of Ordovician conodonts and graptolites from the Argentine Precordillera and western Newfoundland using constrained optimization (CONOP9). In: Stigall, A.L., Hembree, D.I. and Freeman, R.L. (eds) *The Onset of the Great Ordovician Biodiversification Event. Trekking Across the GOBE from the Cambrian through the Katian. Third Annual Meeting of IGCP 653, Athens, Ohio, 2018: Program & Abstracts*, International Geoscience Programme (IGCP), Paris, 25, <http://www.igcp653.org/wp-content/uploads/2018/10/conference-programabstracts.pdf>
- Cashman, P.B. 1990. The affinity of the chitinozoans: new evidence. *Modern Geology*, **15**, 59–69.
- Cashman, P.B. 1991. Lower Devonian chitinozoan juveniles; oldest fossil evidence of a juvenile stage in protists, with an interpretation of their ontogeny and relationship to allogromiid foraminifera. *The Journal of Foraminiferal Research*, **21**, 269–281, <https://doi.org/10.2113/gsjfr.21.3.269>
- Chen, X. 1990. Graptolite depth zonation. *Acta Palaeontologica Sinica*, **29**, 507–526.
- Chen, X. and Bergström, S.M. 1995. *The Base of the austrodentatus Zone as a Level for Global Subdivision of the Ordovician System*. Nanjing University Press, Nanjing, China.
- Chen, X., Zhang, Y.D. and Mitchell, C.E. 2001. Early Darriwilian graptolites from central and western China. *Alcheringa: An Australasian Journal of Paleontology*, **25**, 191–210, <https://doi.org/10.1080/03115510108527805>
- Chen, X., Melchin, M.J., Sheets, H.D., Mitchell, C.E. and Fan, J.X. 2005. Patterns and processes of latest Ordovician graptolite extinction and recovery based on data from south China. *Journal of Paleontology*, **79**, 842–861, [https://doi.org/10.1666/0022-3360\(2005\)079\[0907:UMBFTB\]2.0.CO;2](https://doi.org/10.1666/0022-3360(2005)079[0907:UMBFTB]2.0.CO;2)
- Chen, X., Rong, J.Y. *et al.* 2006. The global boundary stratotype section and point (GSSP) for the base of the Hirnantian Stage (the uppermost of the Ordovician System). *Episodes*, **29**, 183–196, <https://doi.org/10.18814/epiugs/2006/v29i3/004>
- Chen, X., Zhang, Y.D. *et al.* 2017. *Darriwilian to Katian (Ordovician) Graptolites from Northwest China*. Zhejiang University Press, Hangzhou, China [in Chinese].
- Chen, X.H., Zhang, M. and Wang, C.S. 2009. *Ordovician Chitinozoan from South China*. Geological Publishing House, Beijing [in Chinese].
- Collinson, C. and Schwab, H. 1955. *North American Paleozoic Chitinozoa*. Report of Investigations 186. Illinois State Geological Survey, Urbana, IL.
- Cooper, R.A. 1999. The Ordovician time scale – calibration of graptolite and conodont zones. *Acta Universitatis Carolinae – Geologica*, **43**, 1–4.

Ordovician biozonation

- Cooper, R.A. and Lindholm, K. 1990. A precise worldwide correlation of Early Ordovician graptolite sequences. *Geological Magazine*, **127**, 497–525, <https://doi.org/10.1017/S0016756800015429>
- Cooper, R.A. and Sadler, P.M. 2012. The Ordovician Period. In: Gradstein, F.M., Ogg, J.G., Schmitz, M.D. and Ogg, G.M. (eds) *The Geologic Time Scale*. Elsevier, Amsterdam, 489–523.
- Cooper, R.A., Fortey, R.A. and Lindholm, K. 1991. Latitudinal and depth zonation of early Ordovician graptolites. *Lethaia*, **24**, 199–218, <https://doi.org/10.1111/j.1502-3931.1991.tb01468.x>
- Cooper, R.A., Nowlan, G.S. and Williams, H.S. 2001. Global Stratotype Section and Point for base of the Ordovician System. *Episodes*, **24**, 19–28, <https://doi.org/10.18814/epiugs/2001/v24i1/005>
- Cooper, R.A., Maletz, J., Taylor, L. and Zalasiewicz, J.A. 2004. Estimates of Ordovician mean standing diversity in low, middle and high paleolatitudes. In: Webby, B.D., Paris, F., Droser, M.L. and Percival, I.G. (eds) *The Great Ordovician Biodiversification Event*. Columbia University Press, New York, 281–293.
- Cooper, R.A., Rigby, S., Loydell, D.K. and Bates, D.E.B. 2012. Palaeoecology of the Graptoloidea. *Earth-Science Reviews*, **112**, 23–41, <https://doi.org/10.1016/j.earscirev.2012.01.001>
- Cooper, R.A., Sadler, P.M., Munnecke, A. and Crampton, J.S. 2014. Graptoloid evolutionary rates track Ordovician–Silurian global climate change. *Geological Magazine*, **151**, 349–364, <https://doi.org/10.1017/S001675680001198>
- Cooper, R.A., Rigby, S., Bates, D.E.B. and Maletz, J. 2017. Part V, Second Revision, Chapter 6: Paleoecology of the Pterobranchia (Cephalodiscida and Graptolithina). *Treatise Online*, **86**, 1–16, <https://doi.org/10.17161/to.v0i0.6525>
- Crampton, J.S., Meyers, S.R., Cooper, R.A., Sadler, P.M., Foote, M. and Harte, D. 2018. Pacing of Paleozoic macroevolutionary rates by Milankovitch grand cycles. *Proceedings of the National Academy of Sciences of the United States of America*, **115**, 5686–5691, <https://doi.org/10.1073/pnas.1714342115>
- Donoghue, P.C.J., Forey, P.L. and Aldridge, R.J. 2000. Conodont affinity and chordate phylogeny. *Biological Reviews*, **75**, 191–251, <https://doi.org/10.1017/S0016323199005472>
- Donoghue, P.C.J., Purnell, M.A., Aldridge, R.J. and Zhang, S. 2008. The interrelationships of ‘complex’ conodonts (Vertebrata). *Journal of Systematic Palaeontology*, **6**, 119–153, <https://doi.org/10.1017/S1477201907002234>
- Edwards, L.E. 1995. Graphic correlation: Some guidelines on theory and practice and how they relate to reality. *SEPM Special Publications*, **53**, <https://doi.org/10.2110/pec.95.53.0045>
- Eisenack, A. 1931. Neue Mikrofossilien des baltischen Silurs. I. *Paläontologische Zeitschrift*, **13**, 74–118, <https://doi.org/10.1007/BF03043326> [in German].
- Eisenack, A. 1932. Neue Mikrofossilien des baltischen Silurs. II. *Paläontologische Zeitschrift*, **14**, 257–277, <https://doi.org/10.1007/BF03042096> [in German].
- Finney, S.C. 1977. *Graptolites of the Middle Ordovician Athens Shale, Alabama*. PhD thesis, Ohio State University, Columbus, Ohio, USA.
- Finney, S.C. 1986. Graptolite biofacies and correlation of eustatic, subsidence, and tectonic events in the Middle to Upper Ordovician of North America. *Palaios*, **1**, 435–461, <https://doi.org/10.2307/3514628>
- Finney, S.C. and Berry, W.B.N. 1997. New perspectives on graptolite distributions and their use as indicators of platform margin dynamics. *Geology*, **25**, 919–922, [https://doi.org/10.1130/0091-7613\(1997\)025<0919:NPOGDA>2.3.CO;2](https://doi.org/10.1130/0091-7613(1997)025<0919:NPOGDA>2.3.CO;2)
- Finney, S.C., Berry, W.B.N. and Cooper, J.D. 2007. The influence of denitrifying seawater on graptolite extinction and diversification during the Hirnantian (latest Ordovician) mass extinction event. *Lethaia*, **40**, 281–291, <https://doi.org/10.1111/j.1502-3931.2007.00027.x>
- Foote, M., Sadler, P.M., Cooper, R.A. and Crampton, J.S. 2019. Completeness of the known graptoloid paleontological record. *Journal of the Geological Society, London*, **176**, 1038–1055, <https://doi.org/10.1144/gsjgs2019-061>
- Fortey, R.A. and Cocks, L.R.M. 1986. Marginal faunal belts and their structural implications, with examples from the Lower Palaeozoic. *Journal of the Geological Society, London*, **143**, 151–160, <https://doi.org/10.1144/gsjgs.143.1.0151>
- Fortey, R.A., Harper, D.A.T., Ingham, J.K., Owen, A.W. and Rushton, A.W.A. 1995. A revision of Ordovician series and stages from the historical type area. *Geological Magazine*, **132**, 15–30, <https://doi.org/10.1017/S0016756800011390>
- Goldman, D. and Wu, S.Y. 2010. Paleogeographic, paleoceanographic, and tectonic controls on early Late Ordovician graptolite diversity patterns. *Geological Society of America Special Papers*, **466**, 149–161, [https://doi.org/10.1130/2010.2466\(10\)](https://doi.org/10.1130/2010.2466(10))
- Goldman, D., Leslie, S.A., Nölvak, J., Young, S., Bergström, S.M. and Huff, W.D. 2007a. The global stratotype section and point (GSSP) for the base of the Katian Stage of the Upper Ordovician Series at Black Knob Ridge, southeastern Oklahoma, USA. *Episodes*, **30**, 258–270, <https://doi.org/10.18814/epiugs/2007/v30i4/002>
- Goldman, D., Mitchell, C.E., Maletz, J., Riva, J.F.V., Leslie, S.A. and Motz, G.J. 2007b. Ordovician graptolites and conodonts of the Trail Creek Region of central Idaho: a revised, integrated biostratigraphy. *Acta Palaeontologica Sinica*, **46**(Suppl.), 155–162.
- Goldman, D., Podhalńska, T., Sheets, H.D., Bergström, S.M., Nölvak, J. and Reinhart, K. 2012. High resolution stratigraphic correlation and biodiversity dynamics of middle and late Ordovician marine fossils from Poland and Baltoscandia. In: *GeoShale 2012: Recent Advances in Geology of Fine Grained Sediments, Abstracts and Field Trip Guidebook*. Polish Geological Institute and National Research Institute, Warsaw, 35.
- Goldman, D., Sheets, H.D., Bergström, S.M., Nölvak, J., Podhalńska, T., Mitchell, C.E. and Vandebroucke, T.R.A. 2013. High-resolution stratigraphic correlation and biodiversity dynamics of Middle and Late Ordovician marine fossils from Baltoscandia and Poland. *Geological Society of America Abstracts with Programs*, **45**, 236.
- Goldman, D., Nölvak, J. and Maletz, J. 2015. Mid to Late Ordovician graptolite and chitinozoan biostratigraphy of the Kandava-25 drill core in western Latvia. *GFF*, **137**, 1–12.

D. Goldman *et al.*

- 137**, 197–211, <https://doi.org/10.1080/11035897.2015.1021375>
- Goldman, D., Sadler, P.M. and Leslie, S.A. 2020. The Ordovician Period. In: Gradstein, F., Ogg, J.G., Schmitz, M.D. and Ogg, G.M. (eds) *The Geologic Time Scale*. Elsevier, Amsterdam, 631–694.
- Gradstein, F., Ogg, J.G., Schmitz, M.D. and Ogg, G.M. (eds) 2020. *The Geologic Time Scale*. Elsevier, Amsterdam.
- Grahn, Y. 1980. *Early Ordovician Chitinozoa from Öland*. Sveriges Geologiska Undersökning, Serie C, **775**.
- Grahn, Y. and Nölvak, J. 2007. Ordovician Chitinozoa and biostratigraphy from Skåne and Bornholm, southernmost Scandinavia – an overview and update. *Bulletin of Geosciences*, **82**, 11–26, <https://doi.org/10.3140/bull.geosci.2007.01.11>
- Grahn, Y. and Paris, F. 2011. Emergence, biodiversification and extinction of the chitinozoan group. *Geological Magazine*, **148**, 226–236, <https://doi.org/10.1017/S001675681000052X>
- Gutiérrez-Marco, J.C. and Martin, E.L.O. 2016. Biostratigraphy and palaeoecology of Lower Ordovician graptolites from the Fezouata Shale (Moroccan Anti-Atlas). *Palaeogeography, Palaeoclimatology, Palaeoecology*, **460**, 35–49, <https://doi.org/10.1016/j.palaeo.2016.07.026>
- Gutiérrez-Marco, J.C., Sá, A.A., García-Bellido, D.C. and Rábano, I. 2017. The Bohemio-Iberian regional chronostratigraphical scale for the Ordovician System and palaeontological correlations within South Gondwana. *Lethaia*, **50**, 258–295, <https://doi.org/10.1111/let.12197>
- Hall, J. 1859. Notes upon the genus Graptolithus. *Palaeontology of New York*, **3**(Suppl.), 495–529.
- Harper, D.A.T. 2006. The Ordovician biodiversification: Setting an agenda for marine life. *Palaeogeography, Palaeoclimatology, Palaeoecology*, **232**, 148–166, <https://doi.org/10.1016/j.palaeo.2005.07.010>
- Harper, D.A.T., Hammarlund, E.U. and Rasmussen, CMØ. 2014. End Ordovician extinctions: a coincidence of causes. *Gondwana Research*, **25**, 1294–1307, <https://doi.org/10.1016/j.gr.2012.12.021>
- Harris, W.J. and Thomas, D.E. 1938. A revised classification and correlation of the Ordovician graptolite beds of Victoria. *Mining and Geological Journal*, **1**, 62–72.
- Herrera Sánchez, N.C. and Toro, B.A. 2022. First constrained optimization (CONOP9) analyses on Ordovician graptolites from the Central Andean Basin. *Publicación Electrónica de la Asociación Paleontológica Argentina*, **22**, 189–190, <https://doi.org/10.5710/PEAPA.23.03.2022.422>
- Herrera Sánchez, N.C., Toro, B.A. and Lo Valo, G. 2019. Lower–Middle ordovician graptolite biostratigraphy and future challenges for the Central Andean Basin (NW Argentina and S Bolivia). In: Obut, O.T., Sennikov, N.V. and Kipriyanova, T.P. (eds) *13th International Symposium on the Ordovician System: Contributions to the International Symposium*. Publishing House of SB RAS, Novosibirsk, Russia, 71–74.
- Holmden, C., Mitchell, C.E., LaPorte, D.F., Patterson, W.P., Melchin, M.J. and Finney, S.C. 2013. Nd isotope records of late Ordovician sea-level change: Implications for glaciation frequency and global stratigraphic correlation. *Palaeogeography, Palaeoclimatology, Palaeoecology*, **386**, 131–144, <https://doi.org/10.1016/j.palaeo.2013.05.014>
- Jaanusson, V. 1960. Graptolites from the Ontikan and Viruan (Ordovician) limestones of Estonia and Sweden. *Bulletin of the Geological Institutions of the University of Uppsala*, **38**, 289–366.
- Jaanusson, V. 1976. Faunal dynamics in the Middle Ordovician (Viruan) of Baltoscandia. In: Bassett, M.G. (ed.) *The Ordovician System: Proceedings of a Palaeontological Association Symposium Birmingham, September 1974*. University of Wales Press and National Museum of Wales, Cardiff, UK, 301–326.
- Jaanusson, V. 1995. Confacies differentiation and upper Middle Ordovician correlation in the Baltoscandian basin. *Proceedings of the Estonian Academy of Sciences, Geology*, **44**, 73–86.
- Jaglin, J.C. and Paris, F. 1992. Exemples de tétratologie chez les Chitinozoaires du Pridoli de Libye et implications sur la signification biologique du groupe. *Lethaia*, **25**, 151–164, <https://doi.org/10.1111/j.1502-3931.1992.tb01380.x>
- Jenkins, W.A.M. 1969. *Chitinozoa from the Ordovician Viola and Fernvale Limestones of the Arbuckle Mountains Oklahoma*. Special Papers in Palaeontology, **5**.
- Kemple, W.G., Sadler, P.M. and Strauss, D.J. 1995. Extending graphic correlation to many dimensions: Stratigraphic correlation as constrained optimisation. *SEPM Special Publications*, **53**, 65–82, <https://doi.org/10.2110/pec.95.53.0065>
- Klebold, C.J., Leslie, S.A., Goldman, D. and Stouge, S. 2019. Conodont biostratigraphy of the Middle Ordovician (Darriwilian) succession at West Bay Centre Piccadilly Head Quarry, Port Au Port Peninsula, Newfoundland. *Geological Society of America Abstracts with Programs*, **51**, paper 117-7, <https://doi.org/10.1130/abs/2019AM-339107>
- Kozłowski, R. 1963. Sur la nature des Chitinozoaires. *Acta Palaeontologica Polonica*, **8**, 425–449.
- Kraft, P., Storch, P. and Mitchell, C.E. 2015. Graptolites of the Králov Dvůr Formation (mid Katian to earliest Hirnantian, Czech Republic). *Bulletin of Geosciences*, **90**, 195–225, <https://doi.org/10.3140/bull.geosci.1435>
- Leslie, S.A., Goldman, D., Williams, N.A., Derose, L.M. and Hawkins, A.D. 2008. Bedding plane co-occurrence of biostratigraphically useful conodonts and graptolites in Ordovician shale sequences. *Geological Society of America Abstracts with Programs*, **40**, 475.
- Liang, Y. and Tang, P. 2016. Early–Middle Ordovician chitinozoan biostratigraphy of the Upper Yangtze region, South China. *Journal of Stratigraphy*, **40**, 136–150 [in Chinese with English abstract], <https://doi.org/10.19839/j.cnki.dcxzz.2016.02.003>
- Liang, Y., Hints, O., Luan, X.C., Tang, P., Nölvak, J. and Zhan, R.B. 2018. Lower and Middle Ordovician chitinozoans from Honghuayuan, South China: Biodiversity patterns and response to environmental changes. *Palaeogeography, Palaeoclimatology, Palaeoecology*, **500**, 95–105, <https://doi.org/10.1016/j.palaeo.2018.04.002>
- Liang, Y., Bernardo, J., Nölvak, J., Goldman, D., Tang, P. and Hints, O. 2019. Morphological variation suggests that chitinozoans may be fossils of individual microorganisms rather than metazoan eggs. *Proceedings of the Royal Society B: Biological Sciences*, **286**, 20191270, <https://doi.org/10.1098/rspb.2019.1270>

Ordovician biozonation

- Liang, Y., Hints, O. *et al.* 2020. Fossilized reproductive modes reveal a protistan affinity of Chitinozoa. *Geology*, **48**, 1200–1204, <https://doi.org/10.1130/G47865.1>
- Loch, J.D. and Taylor, J.F. 2012. New symphysurinid trilobites from the Cambrian–Ordovician boundary interval in the western United States. *Memoirs of the Association of Australasian Palaeontologists*, **42**, 417–436, <https://search.informit.org/doi/10.3316/informit.98479192982837>
- Locquin, M.V. 1981. Affinités fongiques probables des Chitinozoaires devenant Chitinomycètes. *Cahiers de Micropaléontologie*, **1**, 29–35.
- Löfgren, A. 1993. Conodonts from the lower Ordovician at Hunneberg, south-central Sweden. *Geological Magazine*, **130**, 215–232, <https://doi.org/10.1017/S001675800009870>
- Loydell, D.K. 2012. Graptolite biozone correlation charts. *Geological Magazine*, **149**, 124–132, <https://doi.org/10.1017/S0016756811000513>
- MacDonald, F.A., Karabinos, P.M., Crowley, J.L., Hodgin, E.B., Crockford, P.W. and Delano, J.W. 2017. Bridging the gap between the foreland and hinterland II: Geochronology and tectonic setting of Ordovician magmatism and basin formation on the Laurentian margin of New England and Newfoundland. *American Journal of Science*, **317**, 555–596, <https://doi.org/10.2475/05.2017.02>
- Maletz, J. 2019. Dictyonema Hall and its importance for the evolutionary history of the Graptoloidea. *Palaeontology*, **62**, 151–161, <https://doi.org/10.1111/pala.12394>
- Maletz, J. 2021. Part V, Second Revision, Chapter 7: Biostratigraphy. *Treatise Online*, **146**, 1–22, <https://doi.org/10.17161/to.vi.15162>
- Maletz, J. and Ahlberg, P. 2011. The Lerhamn drill core and its bearing for the graptolite biostratigraphy of the Ordovician Tøyen Shale in Scania, southern Sweden. *Lethaia*, **44**, 350–368, <https://doi.org/10.1111/j.1502-3931.2010.00246.x>
- Maletz, J. and Ahlberg, P. 2018. The Lower Ordovician Tøyen Shale succession in the Fågelsång-3 drill core, Scania, Sweden. *GFF*, **140**, 293–305, <https://doi.org/10.1080/11035897.2018.1470201>
- Maletz, J., Löfgren, A. and Bergström, S.M. 1996. The base of the Tetragraptus approximatus Zone at Mt. Hunneberg, S.W. Sweden: A proposed Global Stratotype for the Base of the Second Series of the Ordovician System. *Newsletters in Stratigraphy*, **34**, 129–159, <https://doi.org/10.1127/nos/34/1996/129>
- Maletz, J., Egenhoff, S. *et al.* 2011. A tale of both sides of Iapetus–upper Darriwilian (Ordovician) graptolite faunal dynamics on the edges of two continents. *Canadian Journal of Earth Sciences*, **48**, 841–859, <https://doi.org/10.1139/e10-105>
- Maletz, J., Wang, X.F. and Wang, C.S. In press. Early Tremadocian (Ordovician) graptolite biostratigraphy and correlation. *Palaeoworld*, <https://doi.org/10.1016/j.palwor.2022.03.010>
- Mauviel, A. and Desrochers, A. 2016. A high-resolution, continuous $\delta^{13}\text{C}$ record spanning the Ordovician–Silurian boundary on Anticosti Island, eastern Canada. *Canadian Journal of Earth Sciences*, **53**, 795–801, <https://doi.org/10.1139/cjes-2016-0003>
- Melchin, M.J. 2008. Restudy of some Ordovician–Silurian boundary graptolites from Anticosti Island, Canada, and their biostratigraphic significance. *Lethaia*, **41**, 155–162, <https://doi.org/10.1111/j.1502-3931.2007.00045.x>
- Melchin, M.J. and Mitchell, C.E. 1991. Late Ordovician extinction in the Graptoloidea. In: Barnes, C.R. and Williams, S.H. (eds) *Advances in Ordovician Geology*. Geological Survey of Canada Papers, **90-9**, 143–156.
- Melchin, M.J., Sadler, P.M. and Cramer, B.D. 2012. The Silurian Period. In: Gradstein, F.M., Ogg, J.G., Schmitz, M.D. and Ogg, G.M. (eds) *The Geologic Time Scale 2020*. Elsevier, Amsterdam, 525–558.
- Melchin, M.J., Mitchell, C.E., Holmden, C. and Štorsch, P. 2013. Environmental changes in the Late Ordovician–Early Silurian: Review and new insights from black shales and nitrogen isotopes. *Geological Society of America Bulletin*, **125**, 1635–1670, <https://doi.org/10.1130/B30812.1>
- Melchin, M.J., Sadler, P.M. and Cramer, B.D. 2020. The Silurian Period. In: Gradstein, F., Ogg, J.G., Schmitz, M.D. and Ogg, G.M. (eds) *The Geologic Time Scale*. Elsevier, Amsterdam, 695–732.
- Miller, F.X. 1977. The graphic correlation method in biostratigraphy. In: Kauffman, E.G. and Hazel, J.E. (eds) *Concepts and Methods of Biostratigraphy*. Dowden, Hutchinson, and Ross, Stroudsburg, PA, 165–186.
- Miller, J.F., Repetski, J.E., Nicoll, R.S., Nowlan, G.S. and Ethington, R.L. 2014. The conodont *Iapetognathus* and its value for defining the base of the Ordovician System. *GFF*, **136**, 185–188, <https://doi.org/10.1080/11035897.2013.862851>
- Miller, J.F., Evans, K.R. *et al.* 2016. Proposed Auxiliary Boundary Stratigraphic Section and Point (ASSP) for the base of the Ordovician System at Lawson Cove, Utah, USA. *Stratigraphy*, **12**, 219–236.
- Mitchell, C.E., Chen, X., Bergström, S.M., Zhang, Y.D., Wang, Z.H., Webby, B.D. and Finney, S.C. 1997. Definition of a global boundary stratotype for the Darriwilian Stage of the Ordovician System. *Episodes*, **20**, 158–166, <https://doi.org/10.18814/epiugs/1997/v20i3/003>
- Mitchell, C.E., Melchin, M.J., Cameron, C.B. and Maletz, J. 2013. Phylogenetic analysis reveals that *Rhabdopleura* is an extant graptolite. *Lethaia*, **46**, 34–56, <https://doi.org/10.1111/j.1502-3931.2012.00319.x>
- Nõlvak, J. and Goldman, D. 2007. Biostratigraphy and taxonomy of three-dimensionally preserved nemagraptids from the Middle and Upper Ordovician of Baltoscandia. *Journal of Paleontology*, **81**, 254–260, [https://doi.org/10.1666/0022-3360\(2007\)81\[254:BATOTP\]2.0.CO;2](https://doi.org/10.1666/0022-3360(2007)81[254:BATOTP]2.0.CO;2)
- Nõlvak, J. and Grahn, Y. 1993. Ordovician chitinozoan zones from Baltoscandia. *Review of Palaeobotany and Palynology*, **79**, 245–269, [https://doi.org/10.1016/0034-6667\(93\)90025-P](https://doi.org/10.1016/0034-6667(93)90025-P)
- Nõlvak, J., Hints, O. and Männik, P. 2006. Ordovician timescale in Estonia: Recent developments. *Proceedings of the Estonian Academy of Sciences, Geology*, **55**, 98–108, <https://doi.org/10.3176/geol.2006.2.02>
- Obut, A.M. 1973. On the geographic distribution, comparative morphology, ecology, phylogeny and systematic position of chitinozoans. In: Zhuravleva, J.T. (ed.) *Environment and Life in the Geological Past*. Nauka, Novosibirsk, USSR, 72–84 [in Russian].
- Paris, F. 1981. *Les Chitinozoaires dans le Paléozoïque du sud-ouest de l'Europe: cadre géologique, étude*

D. Goldman *et al.*

- systématique, biostratigraphie. Mémoires de la Société géologique et minéralogique de Bretagne, **26**.
- Paris, F. 1990. The Ordovician chitinozoan biozones of the Northern Gondwana domain. *Review of Palaeobotany and Palynology*, **66**, 181–209, [https://doi.org/10.1016/0034-6667\(90\)90038-K](https://doi.org/10.1016/0034-6667(90)90038-K)
- Paris, F. 1996. Chitinozoan biostratigraphy and palaeoecology. In: Jansonijs, J. and McGregor, D.C. (eds) *Palynology: Principles and Applications. Volume 2*. American Association of Stratigraphic Palynologists Foundation, College Station, TX, 531–552.
- Paris, F. and Nölvak, J. 1999. Biological interpretation and paleobiodiversity of a cryptic fossil group: the ‘chitinozoan animal’. *Geobios*, **32**, 315–324, [https://doi.org/10.1016/S0016-6995\(99\)80045-X](https://doi.org/10.1016/S0016-6995(99)80045-X)
- Paris, F. and Verniers, J. 2005. Chitinozoa, Microfossils. In: Selly, R.C., Cocks, L.R.M. and Plimer, I. (eds) *Encyclopedia of Geology*. Academic Press, Cambridge, MA, 428–440.
- Paris, F., Achab, A. *et al.* 2004. Chitinozoans. In: Webby, B.D., Paris, F., Droser, M.L. and Percival, I.G. (eds) *The Great Ordovician Biodiversification Event*. Columbia University Press, New York, 281–293.
- Pohl, A., Donnadieu, Y., Le Hir, G., Ladant, J.B., Dumas, C., Alvarez-Solas, J. and Vandebroucke, T.R.A. 2016. Glacial onset predated Late Ordovician climate cooling. *Paleoceanography*, **31**, 800–821, <https://doi.org/10.1002/2016PA002928>
- Pouille, L., Danelian, T. and Maletz, J. 2014. Radiolarian diversity changes during the Late Cambrian–Early Ordovician transition as recorded in the Cow Head Group of Newfoundland (Canada). *Marine Micropaleontology*, **110**, 25–41, <https://doi.org/10.1016/j.marmicro.2013.05.002>
- Reid, P.C. and John, A.W.G. 1981. A possible relationship between chitinozoa and tintinnids. *Review of Palaeobotany and Palynology*, **34**, 251–262, [https://doi.org/10.1016/0034-6667\(81\)90043-9](https://doi.org/10.1016/0034-6667(81)90043-9)
- Rong, J.Y. and Harper, D.A.T. 1988. A global synthesis of latest Ordovician Hirnantian brachiopod faunas. *Transactions of the Royal Society of Edinburgh: Earth Sciences*, **79**, 383–402, <https://doi.org/10.1017/S026359330001436X>
- Rushton, A.W.A. 1982. The biostratigraphy and correlation of the Mertoneth-Tremadoc Series boundary in North Wales. In: Bassett, M.G. and Dean, W.T. (eds) *The Cambrian–Ordovician Boundary: Sections, Fossil Distributions, and Correlations*. National Museum of Wales Geological Series, **3**, 41–59.
- Sadler, P.M. 2003. *Constrained Optimization – Approaches to the Paleobiologic Correlation and Seriation Problems: A Users' Guide and Reference Manual to the CONOP program Family*. Unpublished Report. University of California, Riverside, Riverside, CA.
- Sadler, P.M. 2020. Global composite sections and constrained optimization. In: Gradstein, F.M., Ogg, J.G., Schmitz, M.D. and Ogg, G.M. (eds) *The Geologic Time Scale 2020*. Elsevier, Amsterdam, <https://doi.org/10.1016/B978-0-12-2.00021-8>
- Sadler, P.M. and Cooper, R.A. 2003. Best-fit intervals and consensus sequences; Comparison of the resolving power of traditional biostratigraphy and computer-assisted correlation. In: Harries, P. (ed.) *High Resolution Approaches in Stratigraphic Paleontology*. Kluwer Academic, Dordrecht, The Netherlands, 49–94.
- Sadler, P.M., Cooper, R.A. and Melchin, M.R. 2009. High resolution, early Paleozoic (Ordovician–Silurian) time scales. *Geological Society of America Bulletin*, **121**, 887–906, <https://doi.org/10.1130/B26357.1>
- Sadler, P.M., Cooper, R.A. and Melchin, M.J. 2011. Sequencing the graptolite clade: Building a global diversity curve from local range-charts, regional composites and global time-lines. *Proceedings of the Yorkshire Geological Society*, **58**, 329–343, <https://doi.org/10.1144/pygs.58.4.296>
- Sell, B.K., Leslie, S.A. and Maletz, J. 2011. New U–Pb zircon data for the GSSP for the base of the Katian in Atoka, Oklahoma, USA and the Darriwilian in Newfoundland, Canada. In: Gutiérrez-Marcos, J.C., Rábano, I. and García-Bellido, D. (eds) *Ordovician of the World. Cuadernos del Museo Geominero*, **14**, 537–546.
- Sell, B.K., Ainsaar, L. and Leslie, S.A. 2013. Precise timing of the Late Ordovician (Sandbian) supereruptions and associated environmental, biological, and climatological events. *Journal of the Geological Society, London*, **170**, 711–714, <https://doi.org/10.1144/jgs2012-148>
- Serra, F., Feltes, N.A., Albanesi, G.L. and Goldman, D. 2019. High-resolution conodont biostratigraphy from the Darriwilian Stage (Middle Ordovician) of the Argentine Precordillera and biodiversity analyses: a CONOP9 approach. *Lethaia*, **52**, 188–203, <https://doi.org/10.1111/let.12306>
- Servais, T. and Harper, D.A.T. 2018. The Great Ordovician Biodiversification Event (GOBE): definition, concept and duration. *Lethaia*, **51**, 151–164, <https://doi.org/10.1111/let.12259>
- Servais, T., Molneux, S.G. *et al.* 2017. First Appearance Datums (FADs) of selected acritarch taxa and correlation between Lower and Middle Ordovician stages. *Lethaia*, **51**, 228–253, <https://doi.org/10.1111/let.12248>
- Shaw, A.B. 1964. *Time in Stratigraphy*. McGraw-Hill, New York.
- Sheehan, P.M. 2001. The Late Ordovician mass extinction. *Annual Review of Earth and Planetary Sciences*, **29**, 331–364, <https://doi.org/10.1146/annurev.earth.29.1.331>
- Skevington, D. 1963. A correlation of Ordovician graptolite-bearing sequences. *GFF*, **85**, 298–319.
- Skevington, D. 1973. Ordovician graptolites. In: Hallam, A. (ed.) *Atlas of Palaeobiogeography*. Elsevier, Amsterdam, 27–35.
- Skevington, D. 1974. Controls influencing the composition and distribution of Ordovician graptolite faunal provinces. *Special Papers in Palaeontology*, **13**, 59–73.
- Stouge, S. 2012. Middle Ordovician (late Dapingian–Darriwilian) conodonts from the Cow Head Group and Lower Head Formation, western Newfoundland, Canada. *Canadian Journal of Earth Science*, **49**, 59–90, <https://doi.org/10.1139/e11-057>
- Stouge, S., Bagnoli, G. and McIlroy, D. 2017. *Cambrian–Middle Ordovician Platform-Slope Stratigraphy, Palaeontology and Geochemistry of Western Newfoundland. International Symposium on the Ediacaran–Cambrian Transition Field Trip 2 Guidebook*. Open-File Report NFLD/3325.

Ordovician biozonation

- Sweet, W.C. 1984. Graphic correlation of upper Middle and Upper Ordovician rocks, North American Mid-continent Province, USA. In: Bruton, D.L. (ed.) *Aspects of the Ordovician System*. Paleontological Contributions of the University of Oslo, **295**, 23–35.
- Sweet, W.C. 1988. Mohawkian and Cincinnatian chronostratigraphy. *Bulletin of the New York State Museum*, **462**, 84–90.
- Sweet, W.C. 1995. A conodont-based composite standard for the North American Ordovician: Progress report. In: Cooper, J.D., Droser, M.L. and Finney, S.F. (eds) *Ordovician Odyssey: Short Papers for the Seventh International Symposium on the Ordovician System*. Pacific Section for the Society for Sedimentary Geology (SEPM), Fullerton, CA, 15–20.
- Sweet, W.C. and Bergström, S.M. 1976. Conodont biostratigraphy of the Middle and Upper Ordovician of the United States Midcontinent. In: Bassett, M.G. (ed.) *The Ordovician System: Proceedings of a Palaeontological Association Symposium, Birmingham, September 1974*. University of Wales Press and National Museum of Wales, Cardiff, UK, 121–151.
- Sweet, W.C. and Bergström, S.M. 1984. Conodont provinces and biofacies of the Late Ordovician. *Geological Society of America Special Papers*, **196**, 69–87, <https://doi.org/10.1130/SPE196-p69>
- Terfelt, F., Bagnoli, G. and Stouge, S. 2012. Re-evaluation of the conodont *Iapetognathus* and implications for the base of the Ordovician System GSSP. *Lethaia*, **45**, 227–237, <https://doi.org/10.1111/j.1502-3931.2011.00275.x>
- Thomas, D.E. 1960. The zonal distribution of Australian graptolites. *Journal and Proceedings of the Royal Society of New South Wales*, **94**, 1–58.
- Tolmacheva, T.Y., Degtyarev, K.E. and Ryazantsev, A.V. 2021. Ordovician conodont biostratigraphy, diversity and biogeography in deep-water radiolarian cherts from Kazakhstan. *Palaeogeography, Palaeoclimatology, Palaeoecology*, **578**, 110572, <https://doi.org/10.1016/j.palaeo.2021.110572>
- Toro, B.A. and Herrera Sánchez, N.C. 2019. Stratigraphical distribution of the Ordovician graptolite *Azygograptus* Nicholson & Lapworth in the Central Andean Basin (NW Argentina and S Bolivia). *Comptes Rendus Palevol*, **18**, 493–507, <https://doi.org/10.1016/j.crpv.2019.06.002>
- Toro, B.A. and Maletz, J. 2018. Up-to-date overview of the Ordovician and Silurian graptolites. In: Riglos, M.S., Farjat, A.D. and Pérez Leyton, M.A. (eds) *Fósiles y Facies de Bolivia*. Sincronía Diseño & Publicidad, Santa Cruz de la Sierra, Bolivia, 59–81.
- Toro, B.A., Merlo Arcerito, F.R., Muñoz, D.F., Waisfeld, B.G. and de la Puente, G.S. 2015. Graptolite-trilobite biostratigraphy in the Santa Victoria area, northwestern Argentina. A key for regional and worldwide correlation of the lower Ordovician (Tremadocian – Floian). *Ameghiniana*, **52**, 535–557, <https://doi.org/10.5710/AMGH.16.06.2015.2905>
- Toro, B.A., Heredia, S., Herrera Sánchez, N.C. and Moreno, F. 2020. First Middle Ordovician conodont record related to key graptolites from the western Puna, Argentina: perspectives for an integrated biostratigraphy and correlation of the Central Andean Basin. *Andean Geology*, **47**, 144–161, <https://dx.doi.org/10.5027/andgeoV47n1-3261>
- Vandenbroucke, A.H.M. and Cooper, R.A. 1992. The Ordovician graptolite sequence of Australasia. *Alcheringa: An Australasian Journal of Paleontology*, **16**, 33–65, <https://doi.org/10.1080/03115519208619032>
- Vandenbroucke, T.R.A. 2004. Chitinozoan biostratigraphy of the Upper Ordovician Fågelsång GSSP, Scania, southern Sweden. *Review of Palaeobotany and Palynology*, **130**, 217–239, <https://doi.org/10.1016/j.revpalbo.2003.12.008>
- Vandenbroucke, T.R.A. 2008a. *Upper Ordovician Chitinozoans from the Historical Type Area in the UK*. Monograph of the Palaeontographical Society, **161**, <https://doi.org/10.1080/25761900.2022.12131808>
- Vandenbroucke, T.R.A. 2008b. An Upper Ordovician chitinozoan biozonation in British Avalonia (England, and Wales). *Lethaia*, **41**, 275–294, <https://doi.org/10.1111/j.1502-3931.2007.00090.x>
- Vandenbroucke, T.R.A., Rickards, B. and Verniers, J. 2005. Upper Ordovician chitinozoan biostratigraphy from the type Ashgill area (Cautley district) and the Pus Gill section (Dufton district, Cross Fell Inlier), Cumbria, Northern England. *Geological Magazine*, **142**, 783–807, <https://doi.org/10.1017/S0016756805000944>
- Vandenbroucke, T.R.A., Recourt, P., Nölvak, J. and Nielsen, A.T. 2013. Chitinozoan biostratigraphy of the Late Ordovician *D. clingani* and *P. linearis* graptolite biozones on the Island of Bornholm, Denmark. *Stratigraphy*, **10**, 281–301, <http://www.micropress.org/microaccess/stratigraphy/issue-303/article-1900>
- Wang, C.H., Wang, X.F., Xu, C. and Li, Z.H. 2013. Taxonomy, zonation and correlation of the graptolite fauna across the Lower/Middle Ordovician boundary interval in the Yangtze Gorges area, South China. *Acta Geologica Sinica (English Edition)*, **87**, 32–47, <https://doi.org/10.1111/1755-6724.12028>
- Wang, W.H., Tang, P., Chen, W.J. and Tan, J.Q. 2019. Integrated Lower–Middle Ordovician graptolite and chitinozoan biostratigraphy of the Jiangnan Slope Region, South China. *Palaeoworld*, **28**, 187–197, <https://doi.org/10.1016/j.palwor.2018.06.001>
- Wang, X.F., Stouge, S. et al. 2009. The global stratotype section and point for the Middle Ordovician Series and the Third Stage (Dapingian). *Episodes*, **32**, 96–114, <https://doi.org/10.18814/epiugs/2009/v32i2/003>
- Wang, X.F., Stouge, S. et al. 2021. The Xiaoyangqiao section, Dayangcha, North China: the new global Auxiliary Boundary Stratotype Section and Point (ASSP) for the base of the Ordovician System. *Episodes*, **44**, 359–383, <https://doi.org/10.18814/epiugs/2020/020091>
- Wang, Z.H., Zhen, Y.Y., Bergström, S.M., Wu, R.C., Zhang, Y. and Ma, X. 2019. A new conodont biozone classification of the Ordovician System in South China. *Palaeoworld*, **28**, 173–186, <https://doi.org/10.1016/j.palwor.2018.09.002>
- Webby, B.D. 1995. Towards an Ordovician timescale. In: Cooper, J.D., Droser, M.L. and Finney, S.F. (eds) *Ordovician Odyssey: Short Papers for the Seventh International Symposium on the Ordovician System*. Pacific Section for the Society for Sedimentary Geology (SEPM), Fullerton, CA, 5–9.

D. Goldman *et al.*

- Webby, B.D. 1998. Steps towards a global standard for Ordovician stratigraphy. *Newsletters in Stratigraphy*, **36**, 1–33, <https://doi.org/10.1127/nos/36/1998/1>
- Webby, B.D., Cooper, R.A., Bergström, S.M. and Paris, F. 2004a. Stratigraphic framework and time slices. In: Webby, B.D., Paris, F., Droser, M.L. and Percival, I.G. (eds) *The Great Ordovician Biodiversification Event*. Columbia University Press, New York, 41–47.
- Webby, B.D., Paris, F., Droser, M.L. and Percival, I.G. 2004b. *The Great Ordovician Biodiversification Event*. Columbia University Press, New York.
- Williams, S.H. and Stevens, R.K. 1988. Early Ordovician (Arenig) graptolites from the Cow Head Group, western Newfoundland. *Palaeontographica Canadana*, **5**, 1–167.
- Won, M.-Z., Iams, W.J. and Reed, K. 2005. Earliest Ordovician (Early to Middle Tremadocian) Radiolarian faunas of the Cow Head Group, Western Newfoundland. *Journal of Paleontology*, **79**, 433–459, [https://doi.org/10.1666/0022-3360\(2005\)079<0433:EOETMT>2.0.CO;2](https://doi.org/10.1666/0022-3360(2005)079<0433:EOETMT>2.0.CO;2)
- Zalasiewicz, J.A., Taylor, L., Rushton, A.W.A., Loydell, D.K., Rickards, R.B. and Williams, M. 2009. Graptolites in British stratigraphy. *Geological Magazine*, **146**, 785–850, <https://doi.org/10.1017/S0016756809990434>
- Zhang, Y.D., Zhan, R.B. *et al.* 2019. Ordovician integrative stratigraphy and timescale of China. *Science China Earth Sciences*, **62**, 61–88, <https://doi.org/10.1007/s11430-017-9279-0>
- Zhen, Y.Y. 2021. Middle Ordovician Conodont biostratigraphy of Australasia. *Journal of Earth Science*, **32**, 474–485, <https://doi.org/10.1007/s12583-020-1116-1>
- Zhen, Y.Y. and Nicoll, R.S. 2009. Biogeographic and biostratigraphic implications of the *Serratognathus bilobatus* fauna (Conodonta) from the Emanuel Formation (Early Ordovician) of the Canning Basin, Western Australia. *Records of the Australian Museum*, **61**, 1–30, <https://doi.org/10.3853/j.00067-1975.61.2009.1520>
- Zhen, Y.Y. and Percival, I.G. 2003. Ordovician conodont biogeography – reconsidered. *Lethaia*, **36**, 357–369, <https://doi.org/10.1080/00241160310006402>
- Zhen, Y.Y. and Percival, I.G. 2017. Late Ordovician conodont biozonation of Australia – current status and regional biostratigraphic correlations. *Alcheringa: An Australasian Journal of Paleontology*, **41**, 285–305, <https://doi.org/10.1080/03115518.2017.1282982>
- Zhen, Y.Y., Percival, I.G. and Zhang, Y.D. 2015. Floian (Early Ordovician) conodont-based biostratigraphy and biogeography of the Australasian Superprovince. *Palaeoworld*, **24**, 100–109, <https://doi.org/10.1016/j.palwor.2014.10.011>
- Zhen, Y.Y., Percival, I.G., Normore, L.S. and Dent, L.M. 2017. Floian (Early Ordovician) conodonts of the Canning Basin, Western Australia – biostratigraphy and palaeobiogeographic affinities with Chinese faunas. In: Zhang, Y.D., Zhan, R.B., Fan, J.X. and Muir, L.A. (eds) *Filling the Gap between the Cambrian Explosion and the GOBE – IGCP Project 653 Annual Meeting 2017, Extended Summaries*. Zhejiang University Press, Hangzhou, China, 233–239.
- Zhen, Y.Y., Normore, L.S., Dent, L.M. and Percival, I.G. 2020a. Middle Ordovician (Darriwilian) conodonts from the Goldwyer Formation of the Canning Basin, Western Australia. *Alcheringa: An Australasian Journal of Paleontology*, **44**, 25–55, <https://doi.org/10.1080/03115518.2019.1618915>
- Zhen, Y.Y., Zhang, Y.D., Percival, I.G. and Trigg, S.J. 2020b. Basal Darriwilian graptolites and associated conodonts from New South Wales and their biostratigraphic implications. *Quarterly Notes, Geological Survey of New South Wales*, **153**, 1–17.